Copy No._____

Defence Research and Development Canada
Recherche et développement pour la défense Canada

DEFENCE R&D DÉFENSE

Improvement and Validation of the Trident UNDEX Interface

M.E. Norwood
J. Gregson
Martec Limited

Martec Limited
Suite 400, 1888 Brunswick St.
Halifax, NS
B3J 3J8

Contract Number: W7707-5-3133

Contract Scientific Authority: Dr. M.J. Smith, 902-426-3100 x383

Defence R&D Canada – Atlantic

Contract Report
DRDC Atlantic CR 2006-155
August 2006

Canada

This page intentionally left blank.

Improvement and Validation of the Trident UNDEX Interface

M.E. Norwood
J. Gregson
Martec Limited

Martec Limited
Suite 400, 1888 Brunswick St.
Halifax, NS
B3J 3J8

Contract number: W7707-5-3133

Contract Scientific Authority: Dr. M.J. Smith, 902-426-3100 ext 383

Defence R&D Canada – Atlantic

Contract Report

DRDC Atlantic CR 2006-155

August 2006

Author

M.E. Norwood

Approved by

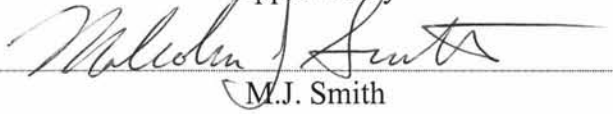

M.J. Smith

Contract Scientific Authority

Approved for release by

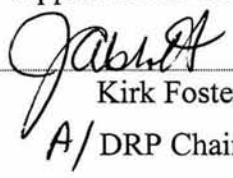

Kirk Foster

A/ DRP Chair

The scientific or technical validity of this Contractor Report is entirely the responsibility of Martec Limited and the contents do not necessarily have the approval or endorsement of DRDC.

Abstract

This technical note provides a summary of work carried out to improve, verify and validate the Trident UNDEX Interface computer code for DRDC. The improvements included the incorporation of a capability to automatically generate, with minimum input from the user, input files for Vast-USA, and a state-of-the-art survey of potential flow methods for calculating the dynamics of near-field UNDEX gas bubbles. The verification and validation focused on the recently developed tightly coupled Vast-USA interface. In total six different problems were investigated for: (1) comparison with the loosely coupled Vast-USA Interface; (2) comparison with LS-DYNA; (3) comparison with experiment; and (4) consistency with units. Recommendations are made for: (1) further improvements to the Trident UNDEX Interface, including the incorporation of a boundary element technique for modeling near-field UNDEX bubble dynamics; and (2) further verification and validation studies.

Résumé

La présente note technique résume les travaux qui ont été menés afin d'améliorer, de vérifier et de valider le code informatique de l'interface Trident UNDEX pour le compte de RDDC. Les améliorations visaient à intégrer une fonction permettant de gérer automatiquement les fichiers d'entrée pour Vast-USA et exigeant un minimum d'intervention de la part de l'utilisateur, ainsi qu'un sondage à la fine pointe de la technologie concernant les méthodes d'écoulement possible, et ce, pour calculer la dynamique des bulles de gaz UNDEX de champ proche. La vérification et la validation étaient axées sur l'interface Vast-USA, qui a été développée récemment et est liée étroitement à l'interface UNDEX. Au total, six problèmes différents ont été examinés, soit : (1) comparaison avec l'interface Vast-USA qui est liée de manière lâche; (2) comparaison avec LS-DYNA; (3) comparaison avec l'expérience; (4) cohérence avec les unités. Les recommandations visent les points suivants : (1) améliorations approfondies de l'interface Trident UNDEX, y compris intégration d'une technique liée à des éléments de contour en vue de modéliser la dynamique des bulles de gaz UNDEX de champ proche; (2) études de vérification et de validation approfondies.

This page intentionally left blank.

Executive summary

Introduction

Simulation of underwater explosion effects on ships and submarines using three-dimensional computer modeling methods is an indispensable tool for naval platform survivability. At DRDC Atlantic, this capability is provided in part through the use of the commercial software Underwater Shock Analysis (USA). As USA does not possess a graphical interface of its own, special software has been developed in the past, with funding from DRDC, for accessing USA through Martec Limited's Trident finite element analysis (FEA) software.

Results

The report describes recent improvements to the Trident interface to USA, including the development of a closely coupled link between Trident and USA. A validation study, which compares simulations obtained with the old and new versions of the Trident/USA interface and by employing different systems of units in the modeling input, indicates that the closely coupled link is the correct functioning. A literature review of boundary element modeling of gas bubble dynamics is also provided.

Significance

The closely coupled link between Trident and USA allows simulations of explosion effects to be performed with improved realism and efficiency. More realistic simulations are possible because structurally non-linear behaviour can now be included in ship and submarine response. Furthermore, efficiency improvements allow simulations to be performed in less time and permit use of more detailed structural models. The boundary element approach to simulating underwater explosion gas bubbles is of interest as it may be considerably less costly than other viable methods for modeling close-proximity bubbles.

Future Plans

Simulations of explosion effects are an important part of survivability assessments being performed for the Maritime Force Protection (MFP) Technology Demonstration Project (TDP). These assessments will use detailed, whole-ship models and will take advantage of the new closely coupled Trident/USA link. The report makes a number of recommendations for further enhancing the interface software, and for implementing a boundary-element based capability for modeling gas bubbles.

Norwood, M.E., and Gregson, J. (2006). Improvement and Validation of the Trident UNDEX Interface. DRDC Atlantic CR 2006-155. Defence R&D Canada – Atlantic.

Sommaire

Introduction

La simulation des effets d'explosions sous-marines sur les navires et les sous-marins à l'aide de méthodes de modélisation informatique tridimensionnelle est indispensable à la survie des plates-formes maritimes. À RDDC Atlantique, cette capacité est assurée au moyen du logiciel commercial Underwater Shock Analysis (USA). Comme USA ne comporte pas sa propre interface graphique, un logiciel spécial a été développé dans le passé, à l'aide de fonds de RDDC, et ce, afin de permettre d'accéder à USA au moyen du logiciel d'analyse d'éléments finis (AEF) Trident de Martec Limited.

Résultats

Le rapport décrit les améliorations qui ont été apportées récemment à l'interface Trident-USA, y compris l'élaboration d'un lien lâche entre ces deux logiciels. Une étude de validation, qui compare les simulations obtenues des ancienne et nouvelle versions de l'interface Trident-USA, et l'emploi de systèmes différents d'unités pour la modélisation indiquent que le lien lâche assure le mode de fonctionnement approprié. Le rapport examine aussi la modélisation des éléments de contour de la dynamique des bulles de gaz.

Pertinence

Le lien lâche entre Trident et USA permet de simuler selon une efficacité et un réalisme accrus les effets d'explosions. D'autres simulations réalistes sont possibles, car le comportement non linéaire sur le plan structural peut maintenant être ajouté à la réponse des navires et des sous-marins. En outre, les améliorations apportés sur le plan de l'efficacité permettre de mener les simulations plus rapidement et de recourir à des modèles structuraux plus détaillés. La démarche faisant appel à des éléments de contour pour les simulations d'explosions sous-marines de bulles de gaz est intéressante dans la mesure où elle peut s'avérer nettement moins onéreuse que d'autres méthodes viables de modélisation des bulles à proximité immédiate.

Plans futurs

Les simulations d'effets d'explosions constituent un aspect important des évaluations en matière de surviabilité qui doivent être menées dans le cadre du Projet de démonstration de la technologie (TDP) de la protection des forces maritimes (MFP). Ces évaluations feront appel à des modèles détaillés de navires complets et tireront profit du nouveau lien lâche Trident-USA. Le rapport fait état d'un certain nombre de recommandations visant l'amélioration approfondie du logiciel d'interface et la mise en œuvre d'une capacité fondée sur les éléments de contour en vue de la modélisation de bulles de gaz.

Norwood, M.E. et Gregson, J. (2006). Improvement and Validation of the Trident UNDEX Interface. RDDC Atlantique CR 2006-155. R & D pour la défense Canada – Atlantique.

Table of Contents

This page intentionally left blank.

1. Introduction

This Technical Note (TN-06-10) provides a summary of the work performed under PWGSC Contract No. W7707-5-3133 entitled “TRIDENT UNDEX INTERFACE”.

The ability to assess the loading, response and survivability of naval structures and equipment to withstand the effects of underwater explosions (UNDEX) is of fundamental importance, particularly for determining the threat damage potential and developing effective counter-measures. In previous contract work with DRDC Atlantic and DRDC Suffield, Martec Limited developed, and incorporated into it’s Trident system, specialized software for calculating UNDEX loading on structures including and interface to the commercial Underwater Shock Analysis (USA) code. Until recently, the USA interface involved USA running in a standalone mode (a loosely coupled link). However, in a recent contract with DRDC Atlantic (W7707-04-2588), Martec developed a new version of the Trident interface to USA that allows Trident’s Vast solver and the USA code to run together in a tightly coupled mode. In this mode, Vast performs the solution, using loads generated by USA. The advantage of this new version is that it now allows for nonlinear response analyses.

The primary purpose of this contract was to verify and validate the new tightly coupled Trident-USA interface using a series of test problems. This has involved comparing results from linear analysis using both loosely coupled and tightly coupled versions, and UNDEX analysis involving shock analysis using doubly asymptotic approximations (DAA) and bubble pulse loading using virtual mass approximations (VMA). The verification and validation carried out in this contract is presented in Section 2.0

The USA code itself consists of several modules, each one executed separately, and requiring separate input data sets. Preparing the latter is most often tedious and error prone. Under this contract, a capability to automatically generate these files – with minimum input from the user – has been implemented in the UNDEX software. This capability is described more fully in Section 3.0.

Although the specialized UNDEX software developed by Martec offers a sufficient capability for dealing with far-field bubble dynamics, such is not the case for the near- field. In recent years potential flow methods for calculating the dynamics of near-field UNDEX gas bubbles have been investigated. As part of this current contract, a survey of the work in this area has been carried out, and recommendations made for future implementation of such a capability into the UNDEX software. The result of this survey is presented in Section 4.0

2. Verification and Validation of the New USA Interface

In all six different problems have been considered for verification and validation. They were: (1) the quarter sphere USA demonstration problem; (2) a full sphere with diaphragm; (3) the quarter cylinder USA demonstration problem; (4) the submerged cylinder problem described in [DeRuntz, 1986]; (5) the CPF; and (6) the Suffield circular test plate problem.

2.1 Quarter Sphere Analysis

The finite element model for the quarter sphere problem is shown in Figure 2.1.1. This analysis uses a plane wave approximation (PWA) to the loading. The magnitude of the loading is such that the sphere responds in a linear manner.

Computed velocity time histories for two nodes, 134 and 235, without damping, using both the tightly-coupled (T-C) and loosely-coupled (L-C) USA interfaces, are shown in Figures 2.1.2 and 2.1.3.

Computed velocity comparisons with mass proportional damping (A Type) are shown in Figures 2.1.4 and 2.1.5. Computed velocity comparisons with stiffness proportional damping (B Type) are shown in Figures 2.1.6 and 2.1.7.

Computed velocity comparisons using English units (inches and pounds) and metric units (millimeters and Newtons) are shown in Figures 2.1.8 and 2.1.9.

In the tightly-coupled USA interface, there is a Vast module for linear analysis (DISP3) and a Vast module for nonlinear analysis (DISP3N). Computed velocity comparisons using DISP3 and DISP3N modules are shown in Figures 2.1.10 and 2.1.11.

Computed velocity comparisons using Vast and LS-Dyna are shown in Figures 2.1.12 and 2.1.13.

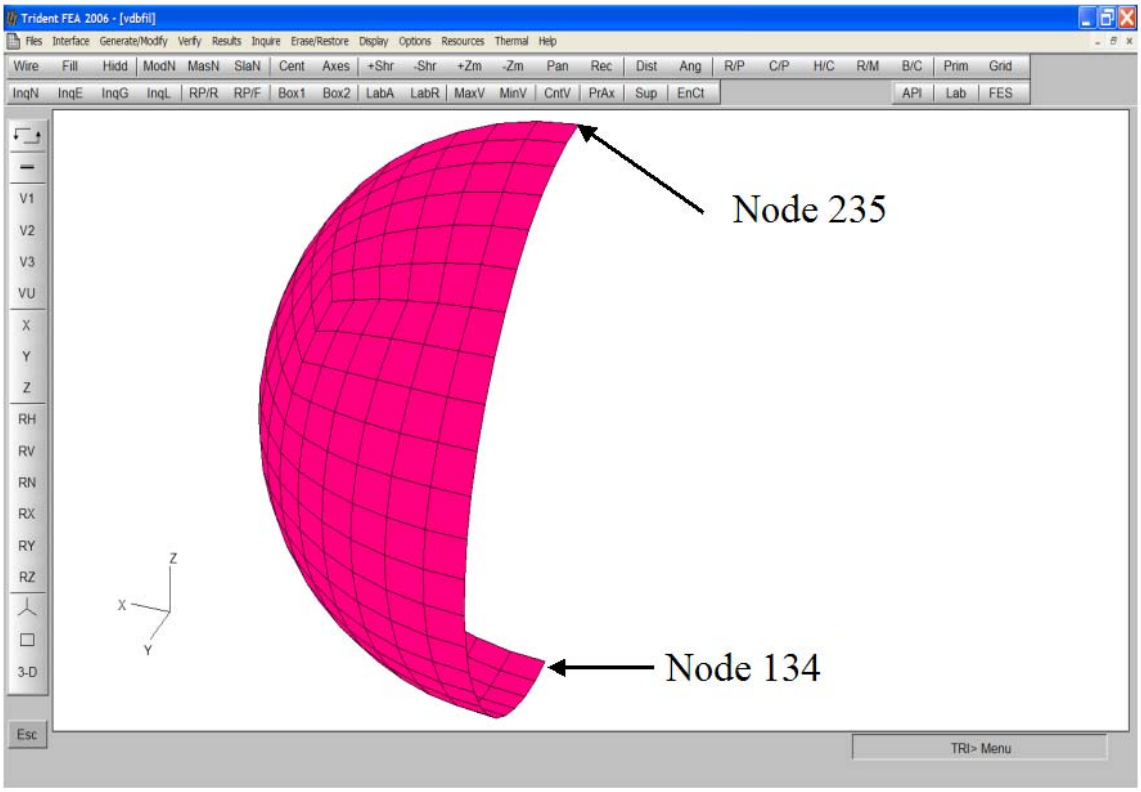

Figure 2.1.1: Trident Finite Element Model of Quarter Sphere

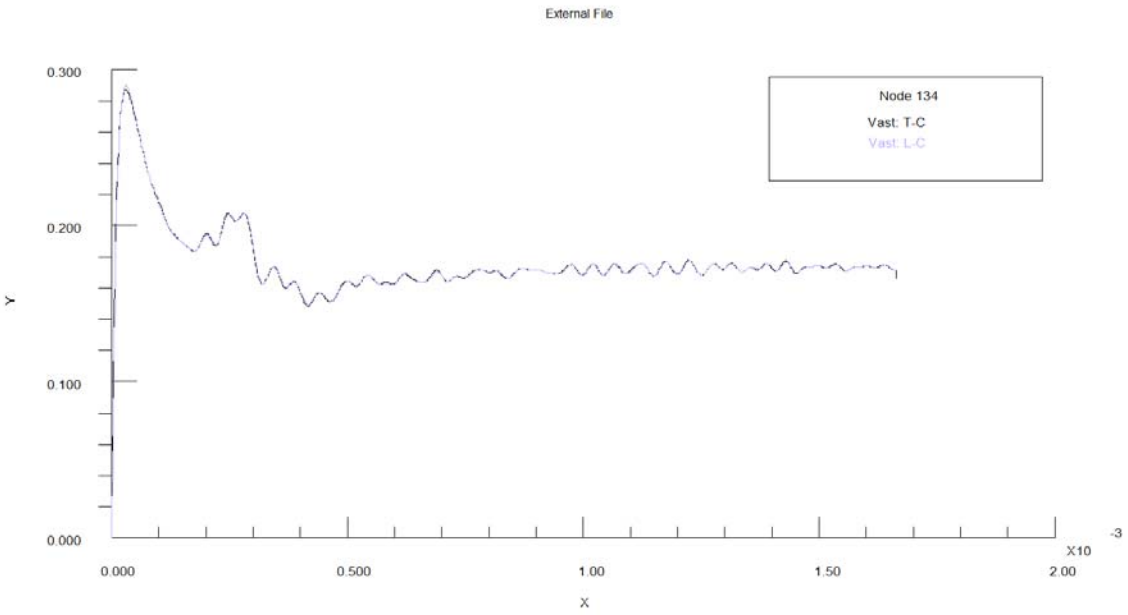

Figure 2.1.2: T-C and L-C Velocity Comparison for Node 134

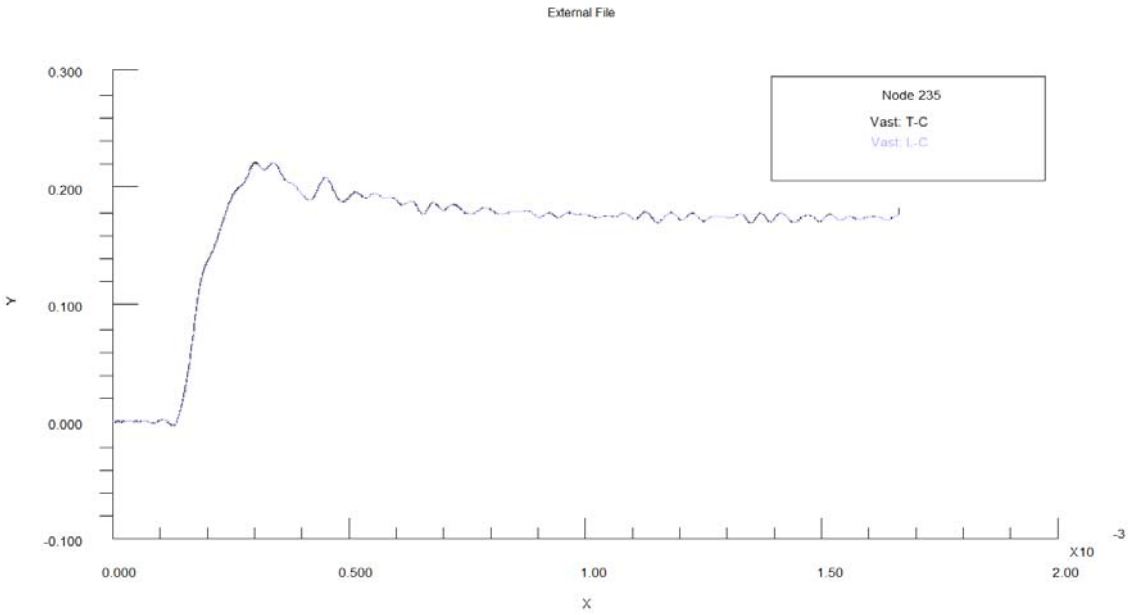

Figure 2.1.3: T-C and L-C Velocity Comparison for Node 235

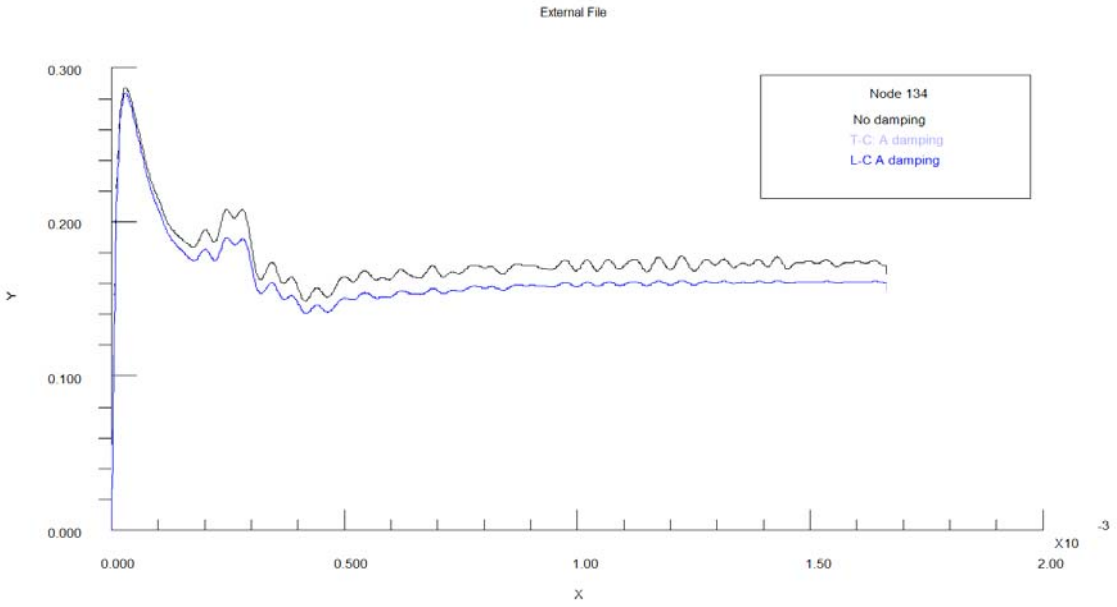

Figure 2.1.4: T-C and L-C Velocity Comparison for Node 134 - With A Type Damping

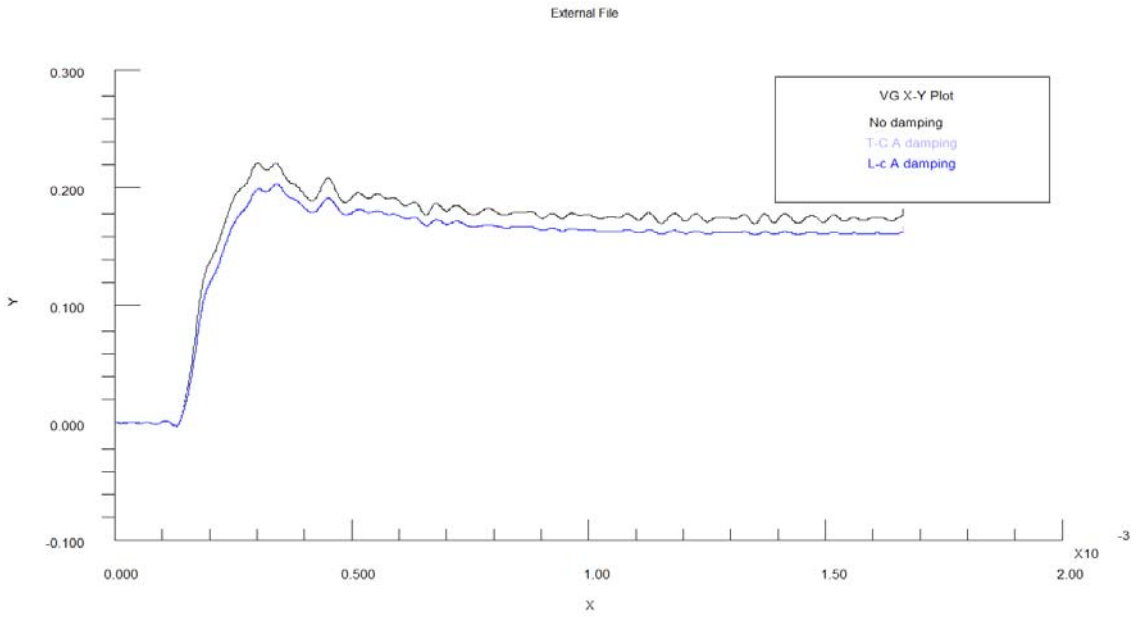

Figure 2.1.5: T-C and L-C Velocity Comparison for Node 235 - With A Type Damping

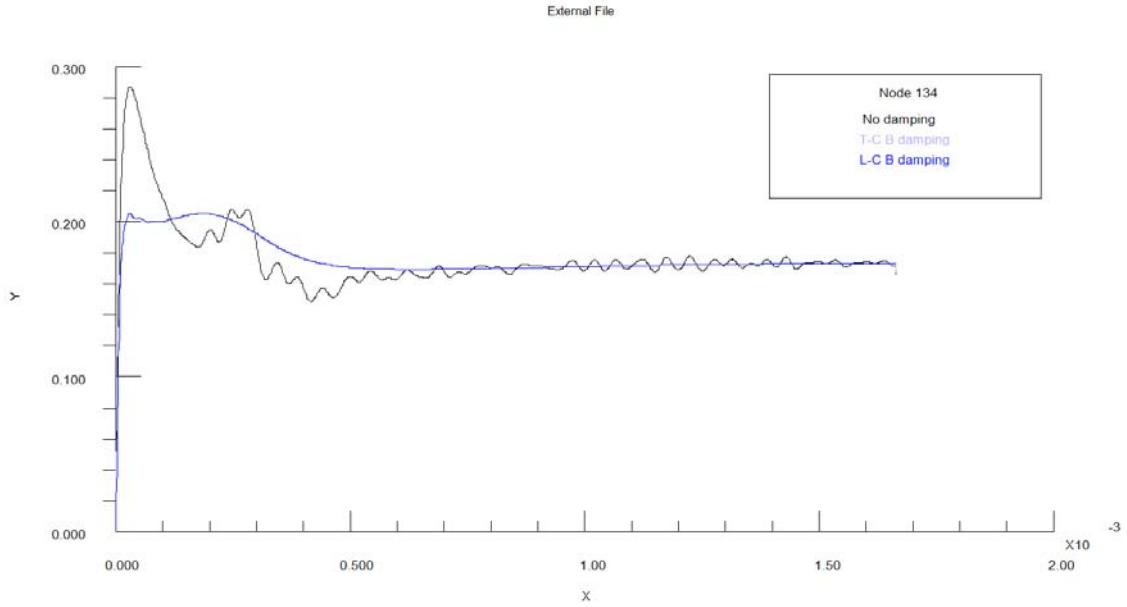

Figure 2.1.6: T-C and L-C Velocity Comparison for Node 134 - With B Type Damping

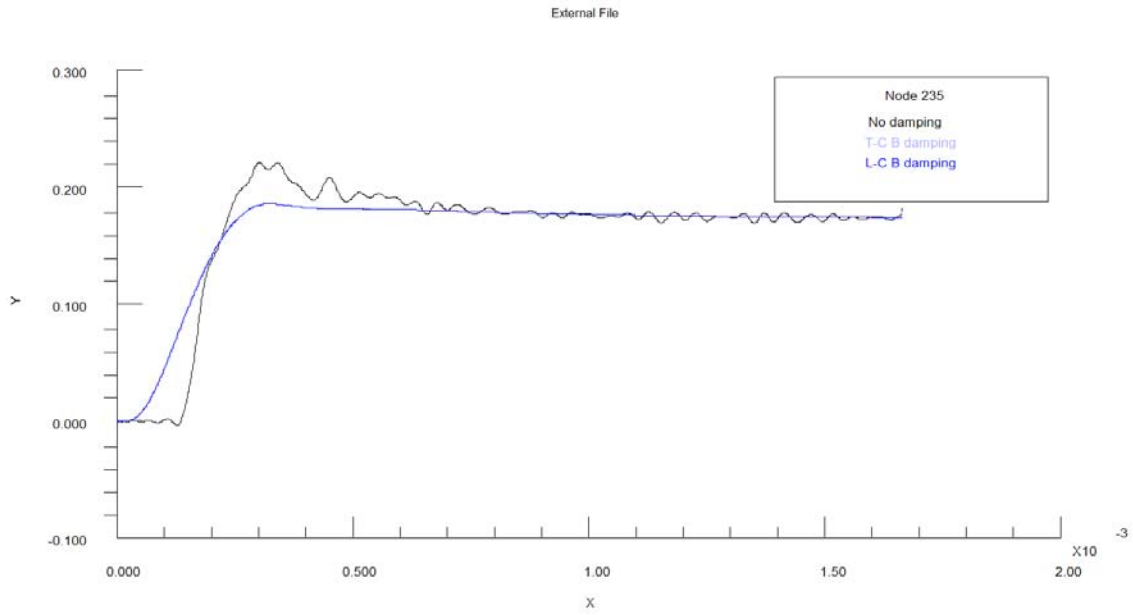

Figure 2.1.7: T-C and L-C Velocity Comparison for Node 235 - With B Type Damping

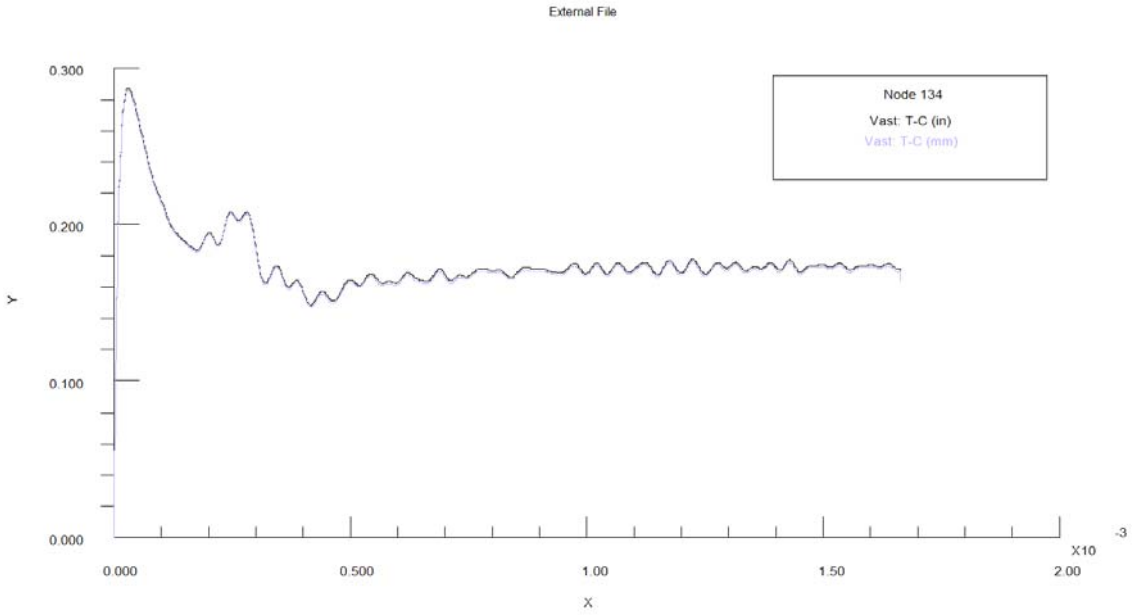

Figure 2.1.8: Velocity Comparison for Node 134 - English Units Versus Metric Units

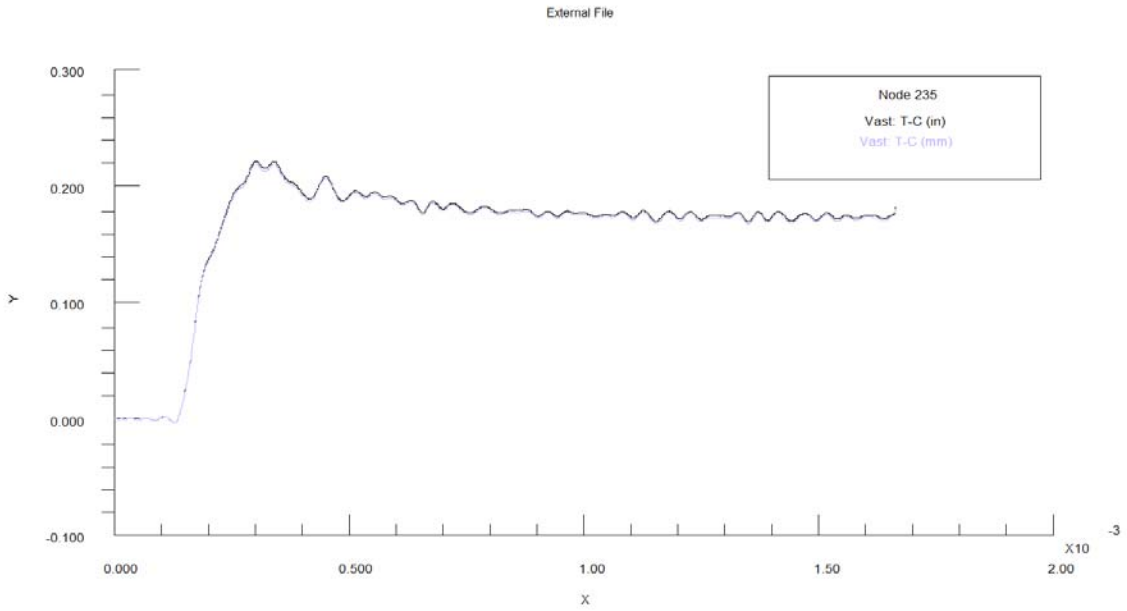

Figure 2.1.9: Velocity Comparison for Node 235 - English Units Versus Metric Units

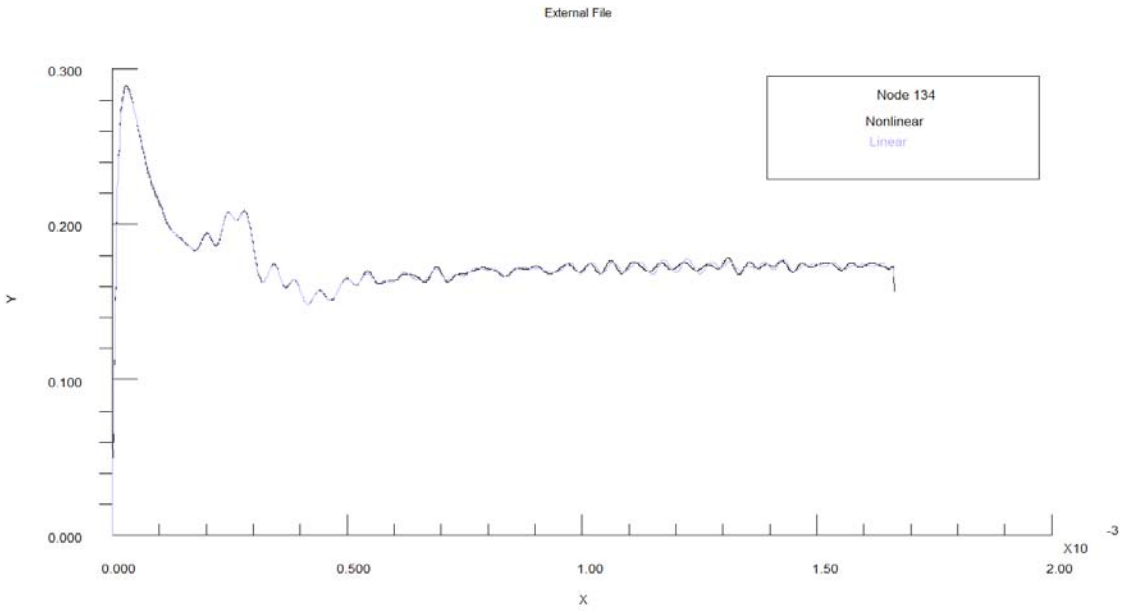

Figure 2.1.10: Velocity Comparison for Node 134 - Linear Module Versus Nonlinear Module

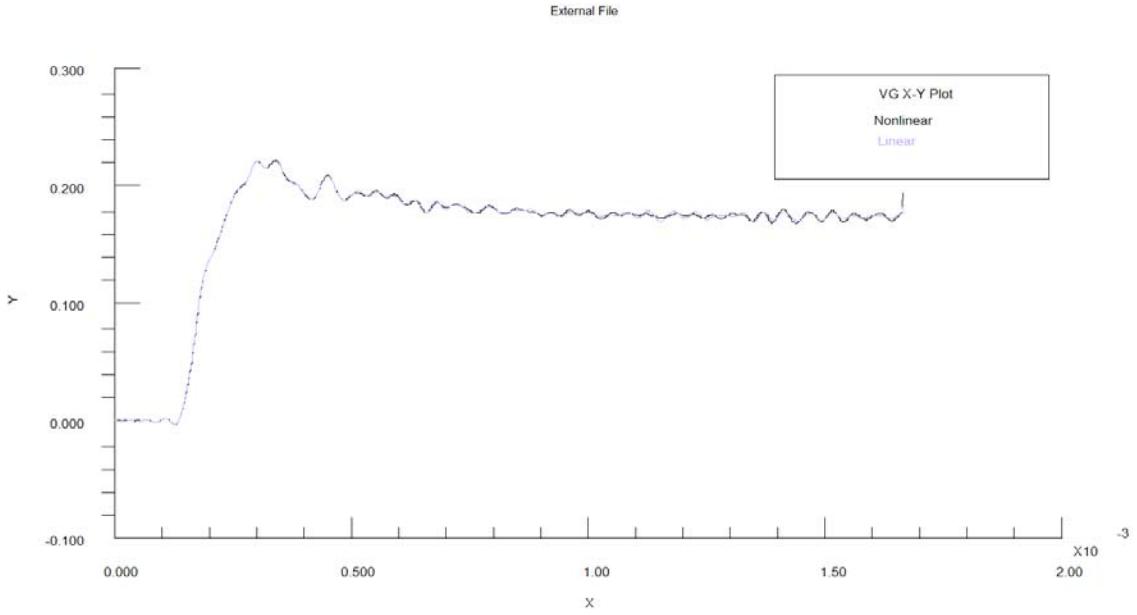

Figure 2.1.11: Velocity Comparison for Node 235 - Linear Module Versus Nonlinear Module

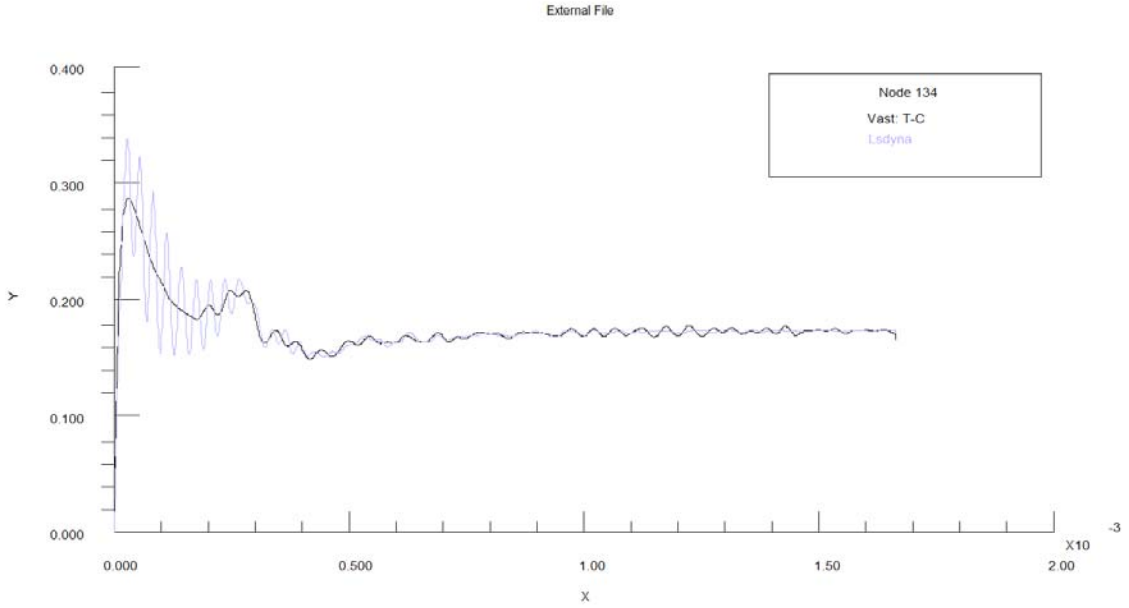

Figure 2.1.12: Velocity Comparison for Node 134 - Vast Versus LS-Dyna

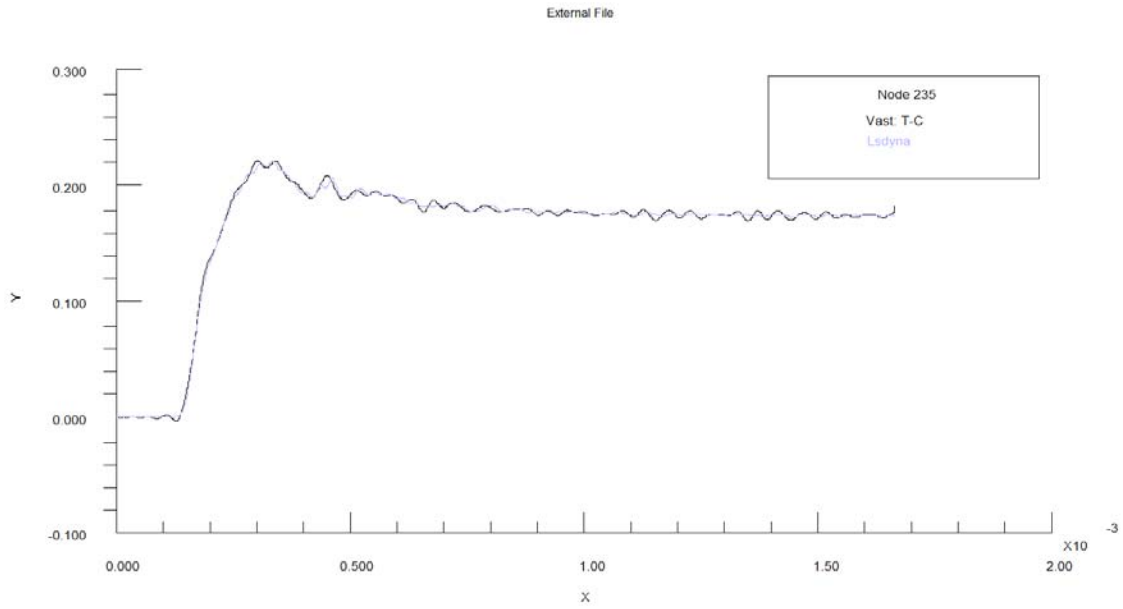

Figure 2.1.13: Velocity Comparison for Node 235 - Vast Versus LS-Dyna

2.2 Sphere with Diaphragm

The quarter sphere model used in Section 2.1 had a one-on-one node and element count for structural and wetted surface elements. The sphere with diaphragm model shown in Figure 2.2.1 represents the typical case where there are more structural elements than wetted surface elements.

Computed velocity time histories for two nodes, 134 and 235, using both the tightly-coupled (T-C) and loosely-coupled (L-C) USA interfaces, are shown in Figures 2.2.2 and 2.2.3.

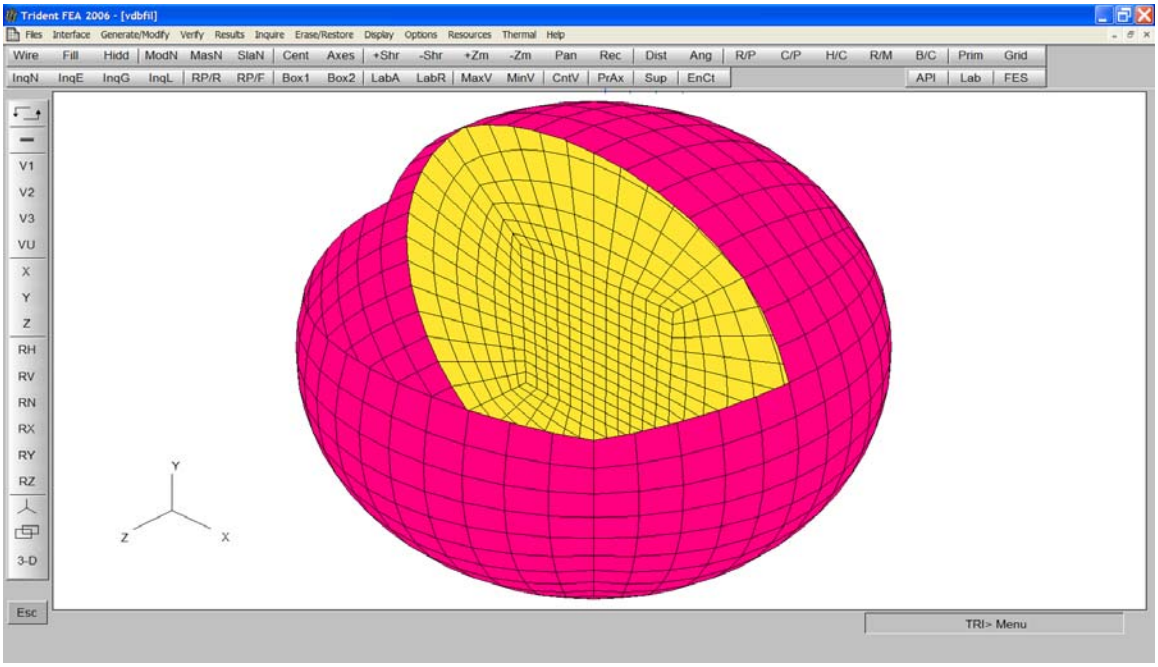

Figure 2.2.1: Trident Finite Element Model of Sphere With Diaphragm

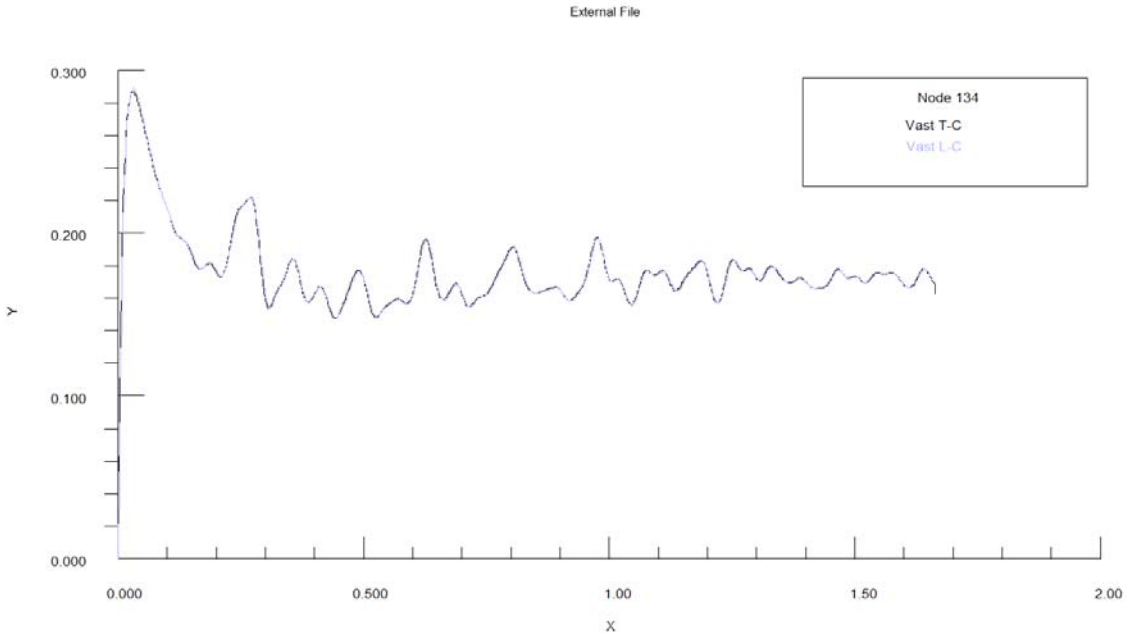

Figure 2.2.2: T-C and L-C Velocity Comparison for Node 134

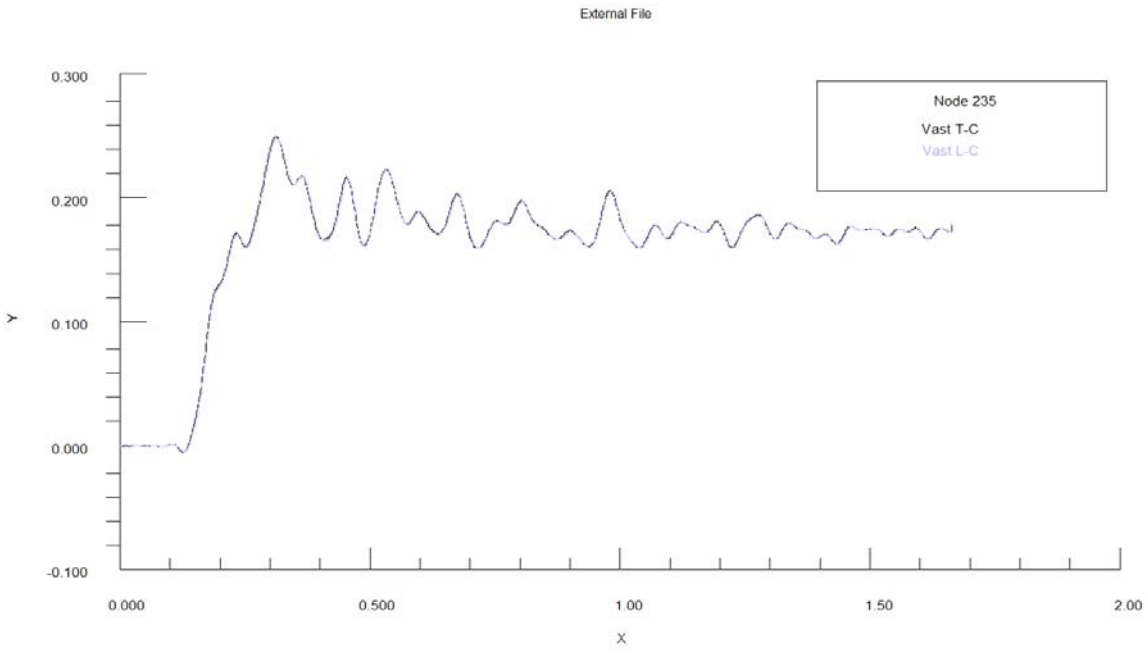

Figure 2.2.3: T-C and L-C Velocity Comparison for Node 235

2.3 Quarter Cylinder Analysis

The finite element model for the quarter cylinder problem is shown in Figure 2.3.1. This analysis uses a doubly asymptotic approximation (DAA1) to a spherical shock wave loading. The magnitude of the loading is such that the cylinder responds in a linear manner.

Computed velocity time histories for two nodes, 1 and 117, using both the tightly-coupled (T-C) and loosely-coupled (L-C) USA interfaces, are shown in Figures 2.3.2 and 2.3.3.

Computed velocity comparisons using English units (inches and pounds) and metric units (millimeters and Newtons) are shown in Figures 2.3.4 and 2.3.5.

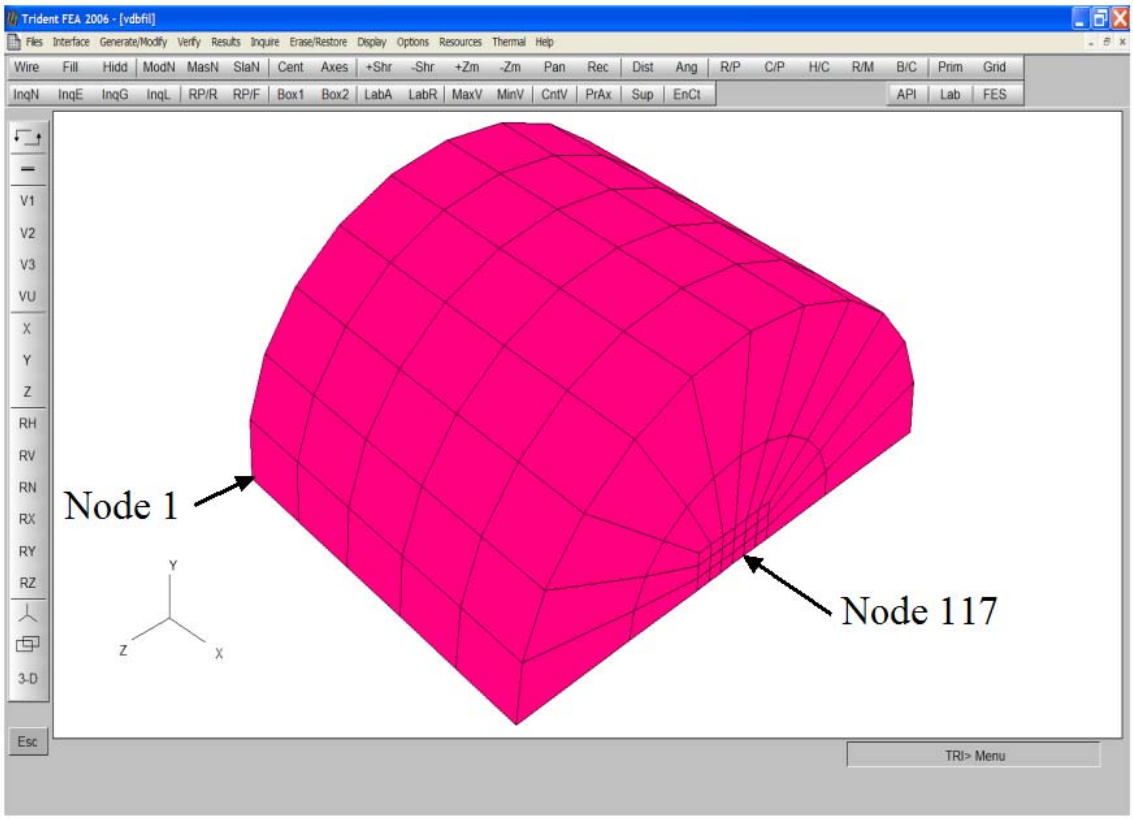

Figure 2.3.1: Trident Finite Element Model of Quarter Cylinder

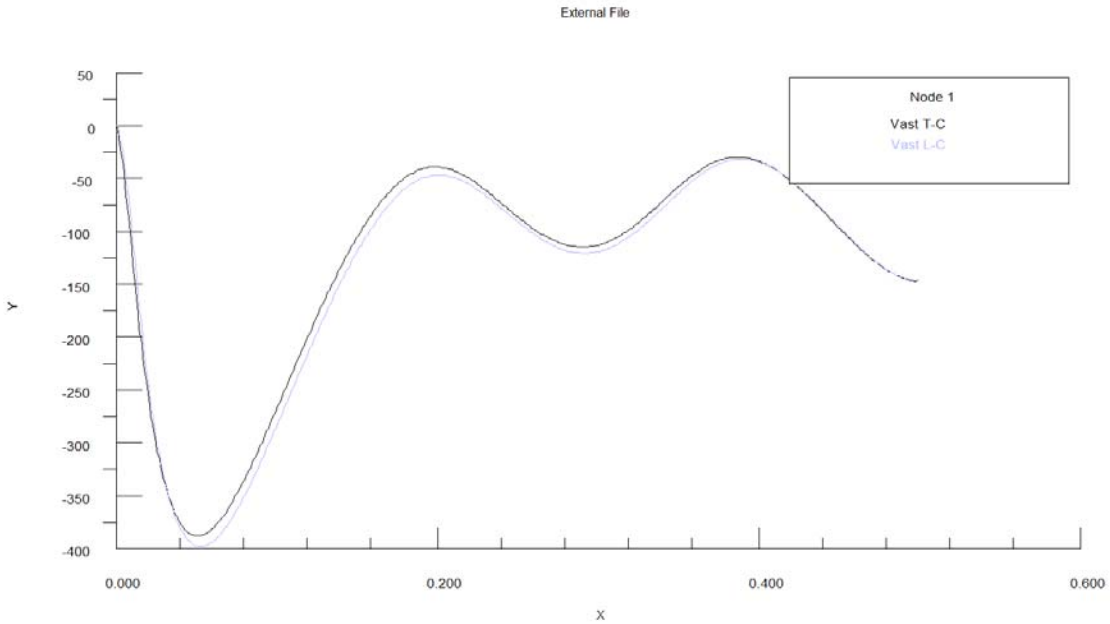

Figure 2.3.2: T-C and L-C Velocity Comparison for Node 1

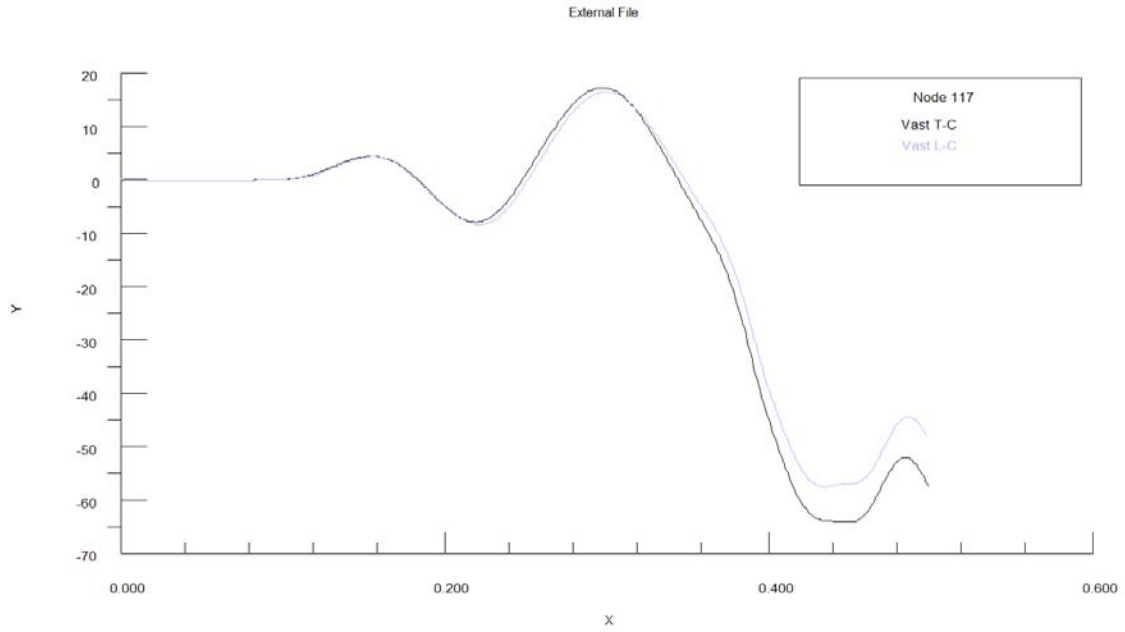

Figure 2.3.3: T-C and L-C Velocity Comparison for Node 117

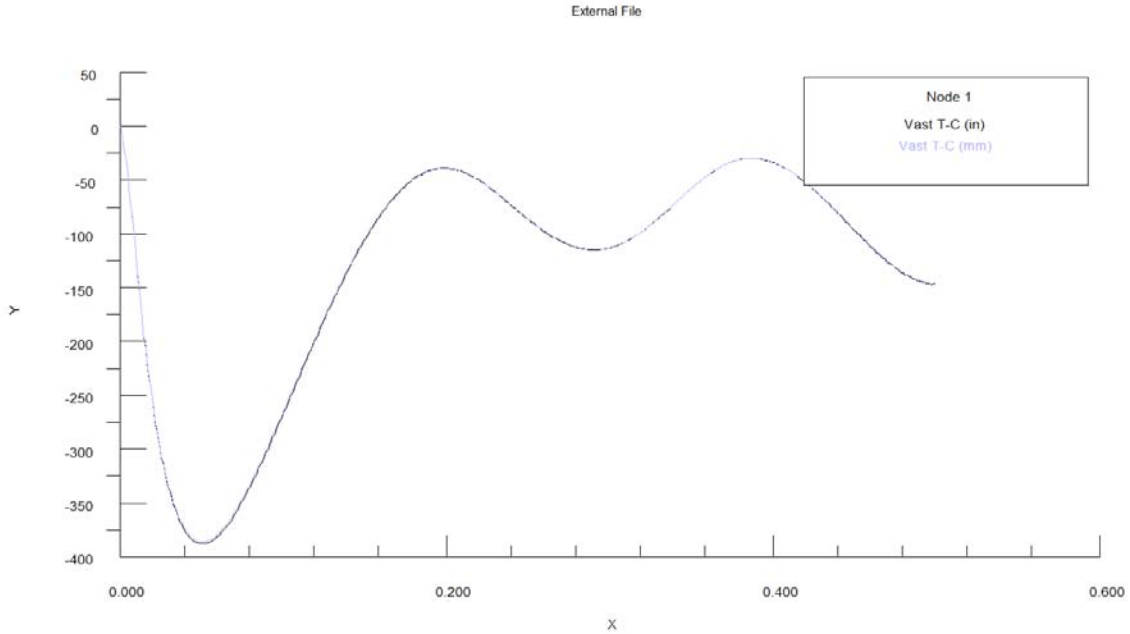

Figure 2.3.4: Velocity Comparison for Node 1 - English Units Versus Metric Units

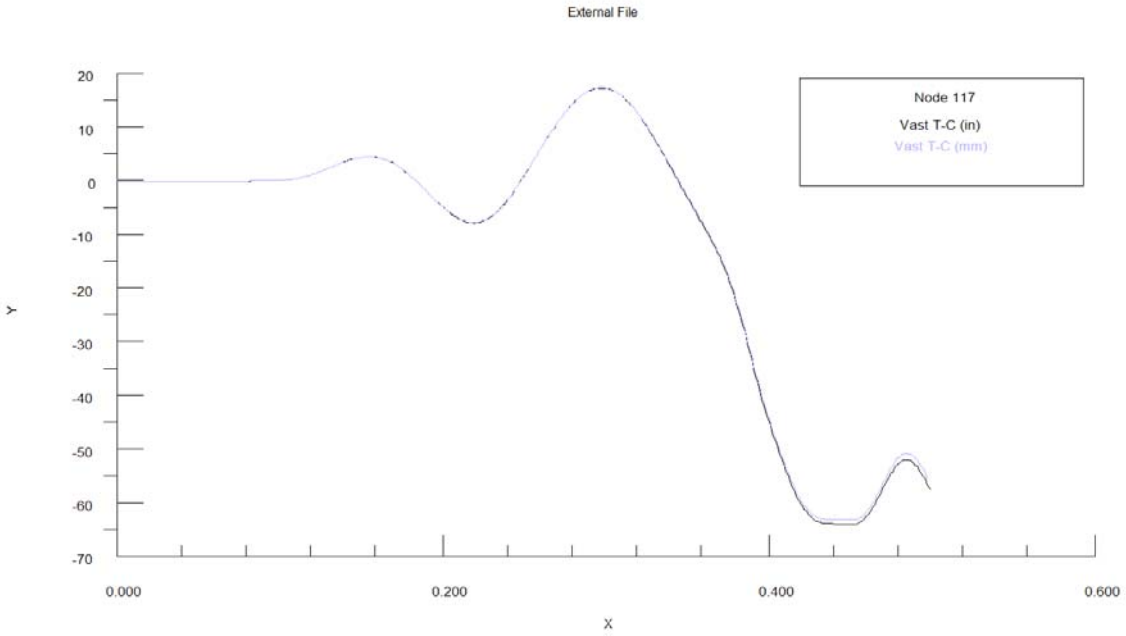

Figure 2.3.5: Velocity Comparison for Node 117 - English Units Versus Metric Units

2.4 Submerged Cylinder Analysis

The finite element model for the submerged cylinder problem is shown in Figures 2.4.1 and 2.4.2. This analysis uses a virtual mass approximation (VMA) to a bubble pulse loading. The magnitude of the loading is such that the cylinder responds in a linear manner. Two types of boundary conditions were considered – unconstrained and pinned.

Computed displacement and velocity time histories for the unconstrained condition, for two nodes, 329 and 169, using both the tightly-coupled (T-C) and loosely-coupled (L-C) USA interfaces, are shown in Figures 2.4.3 to 2.4.6.

Computed displacement and velocity time histories for the pinned condition, for node 169, using both the tightly-coupled (T-C) and loosely-coupled (L-C) USA interfaces are shown in Figures 2.4.7 and 2.4.8.

Computed displacement and velocity comparisons using English units (inches and pounds) and metric units (millimeters and Newtons) are shown in Figures 2.4.9 and 2.4.10.

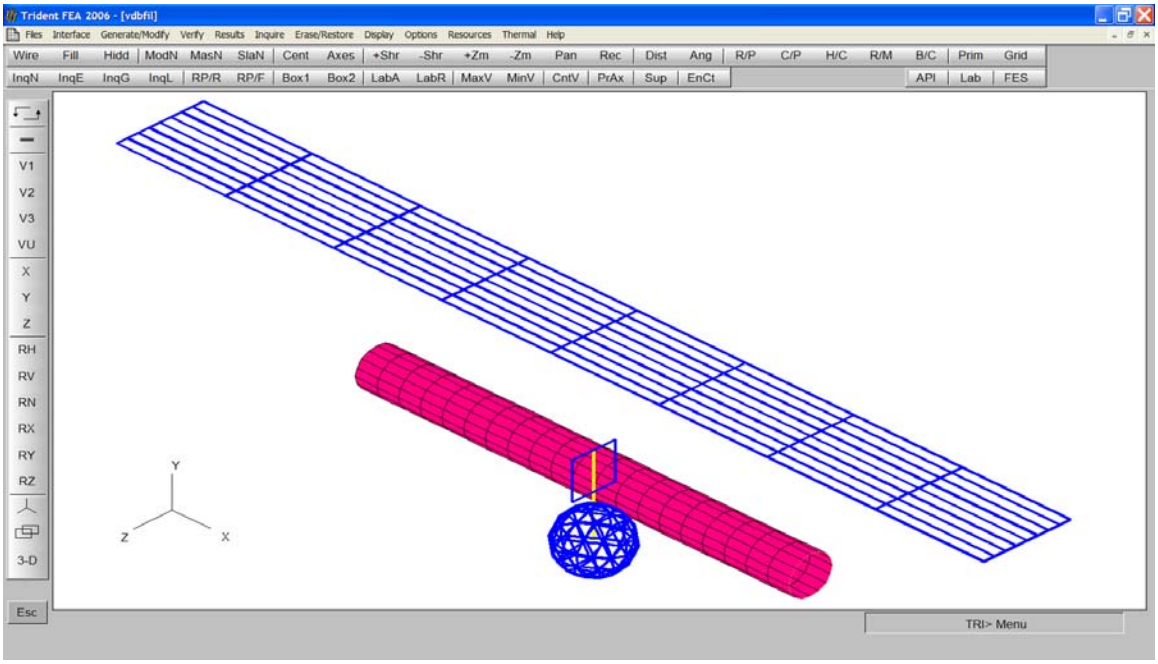

Figure 2.4.1: Trident Finite Element Model of Submerged Cylinder

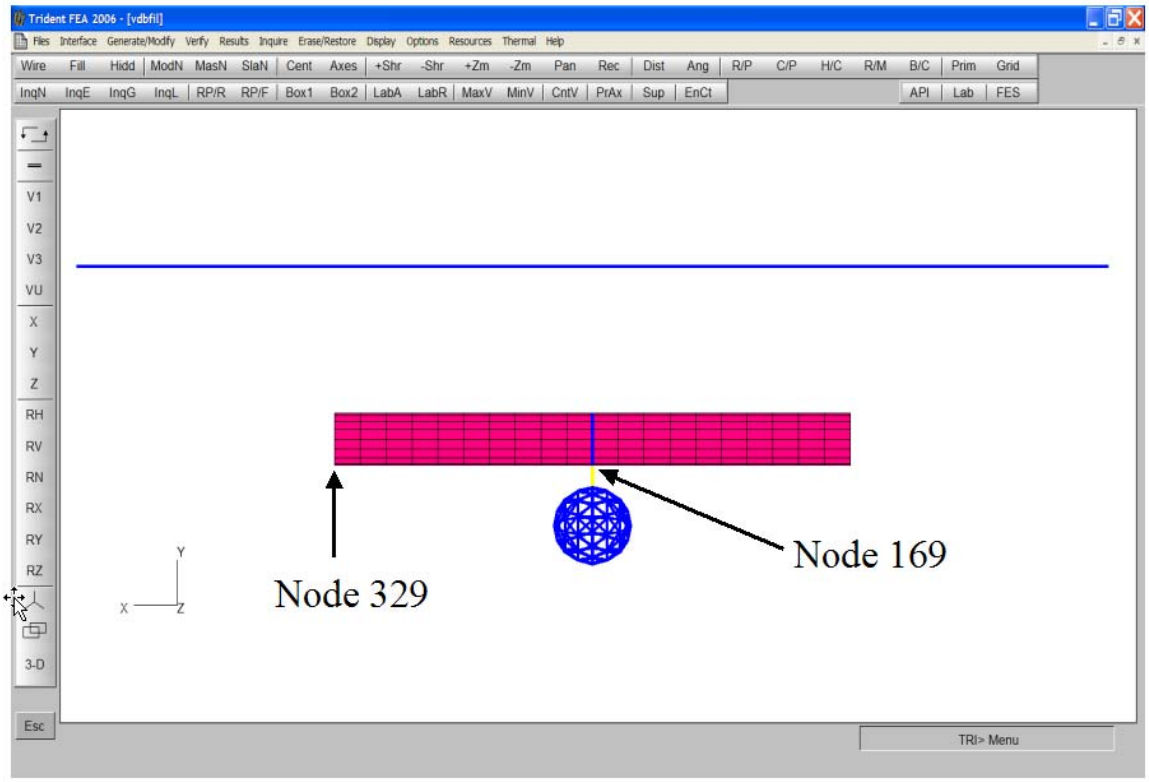

Figure 2.4.2: Trident Finite Element Model of Submerged Cylinder - Side View

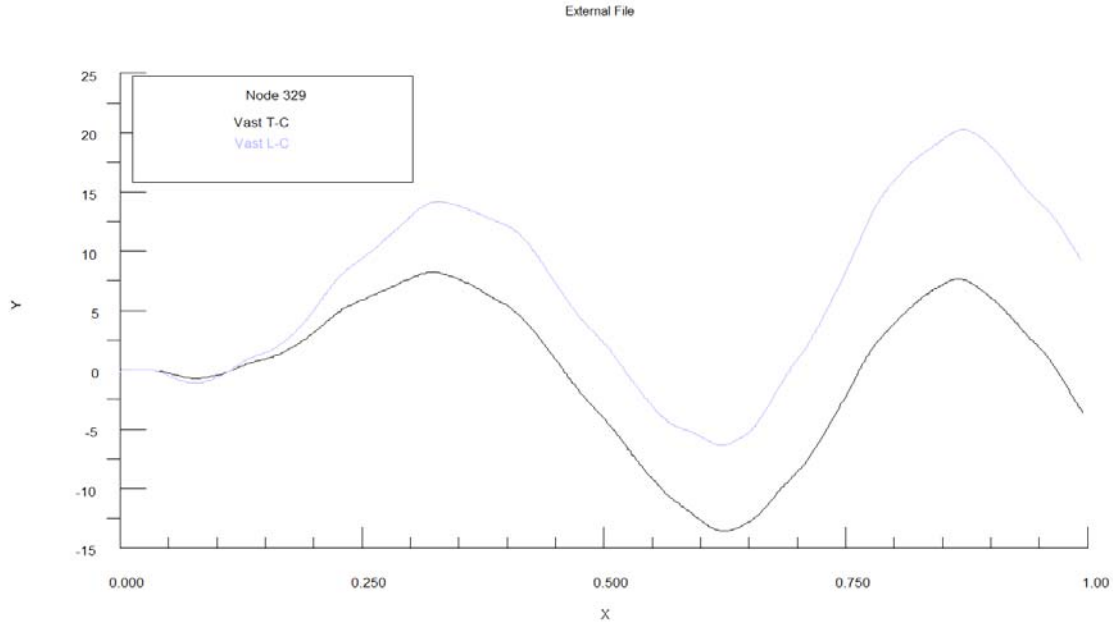

Figure 2.4.3: T-C and L-C Displacement Comparison for Node 329

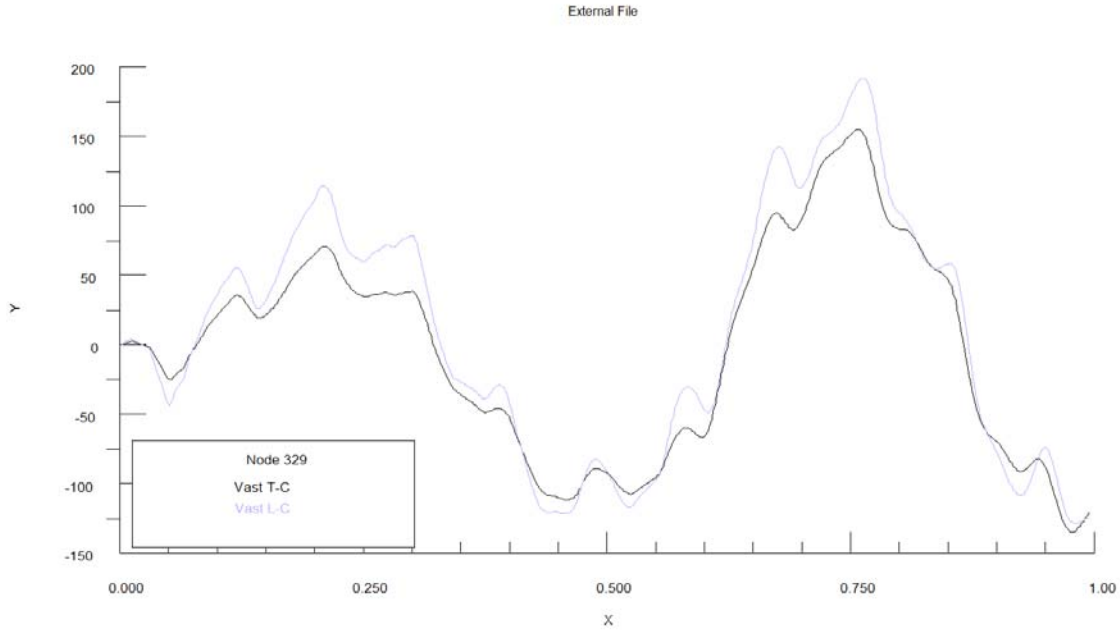

Figure 2.4.4: T-C and L-C Velocity Comparison for Node 329

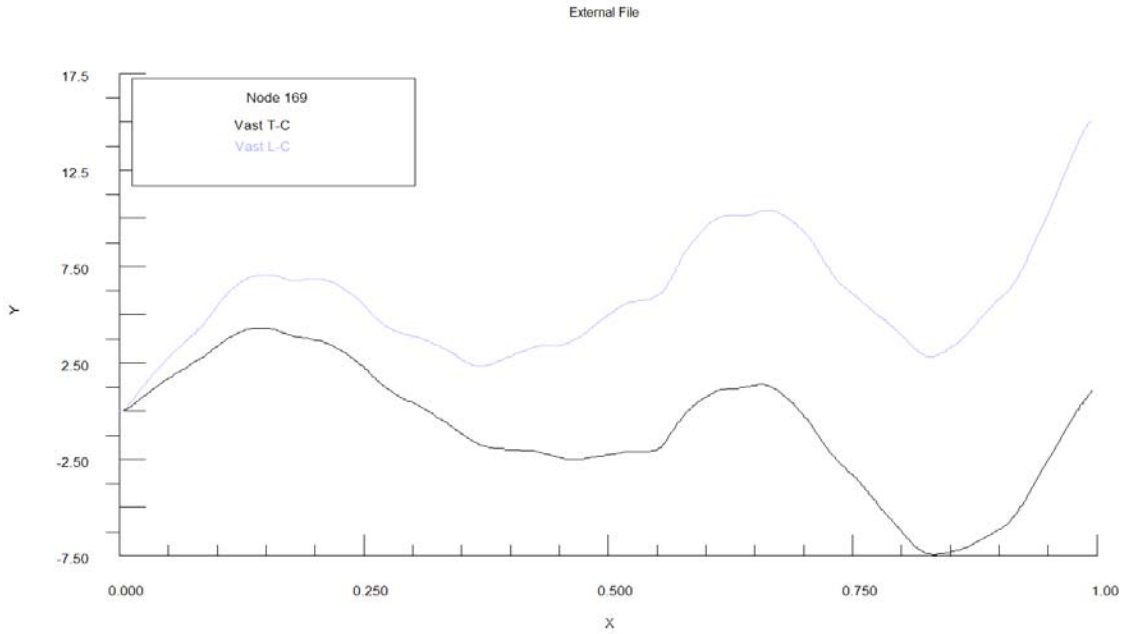

Figure 2.4.5: T-C and L-C Displacement Comparison for Node 169

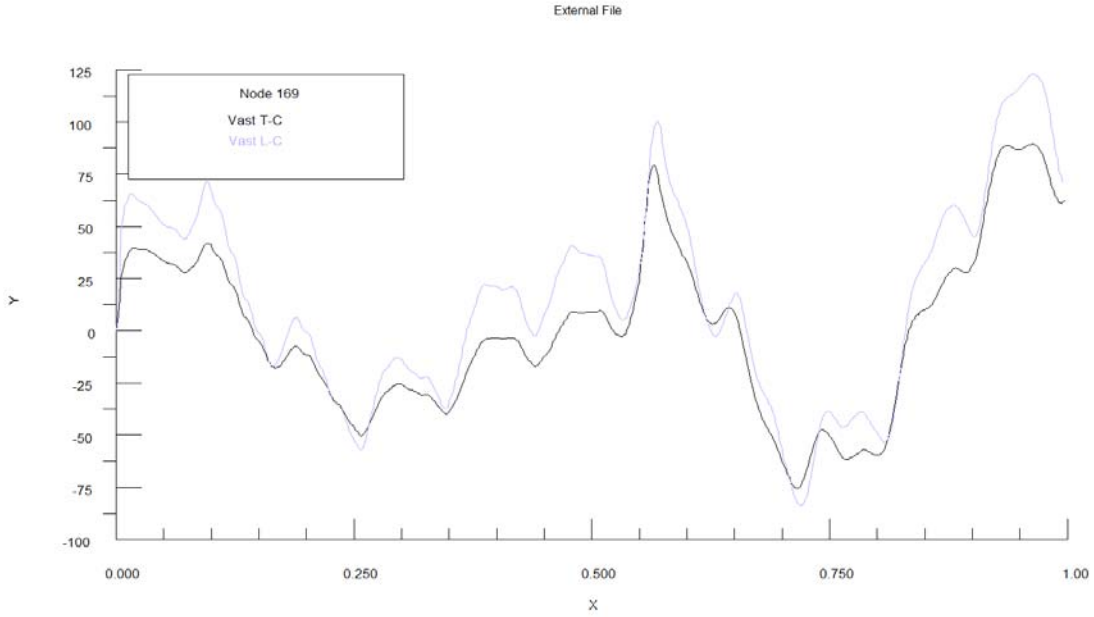

Figure 2.4.6: T-C and L-C Velocity Comparison for Node 169

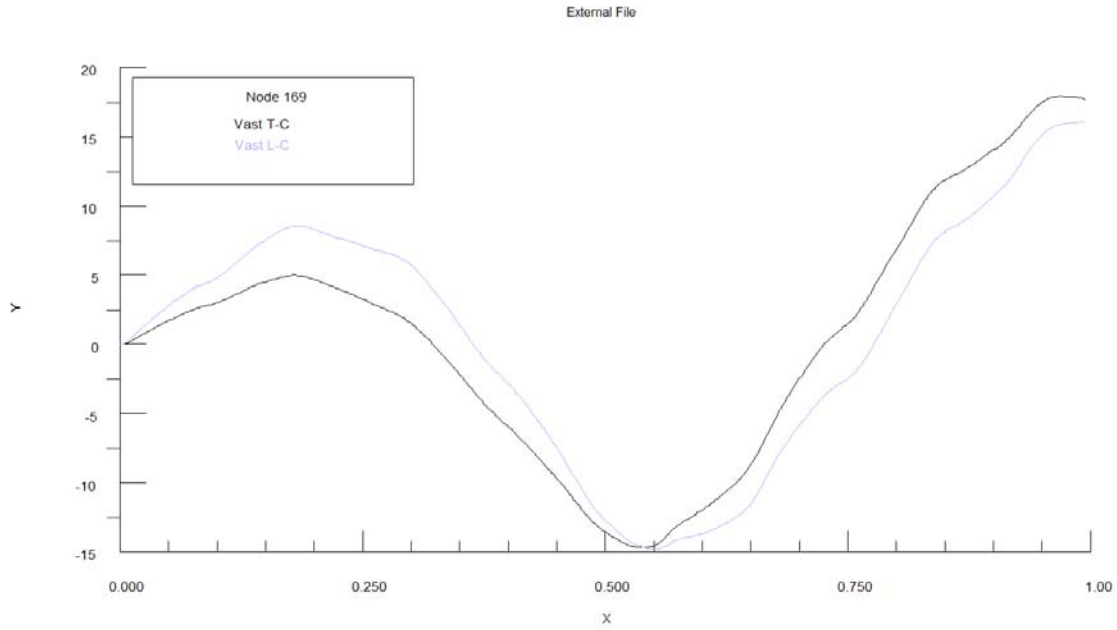

Figure 2.4.7: T-C and L-C Displacement Comparison for Node 169 - Pinned

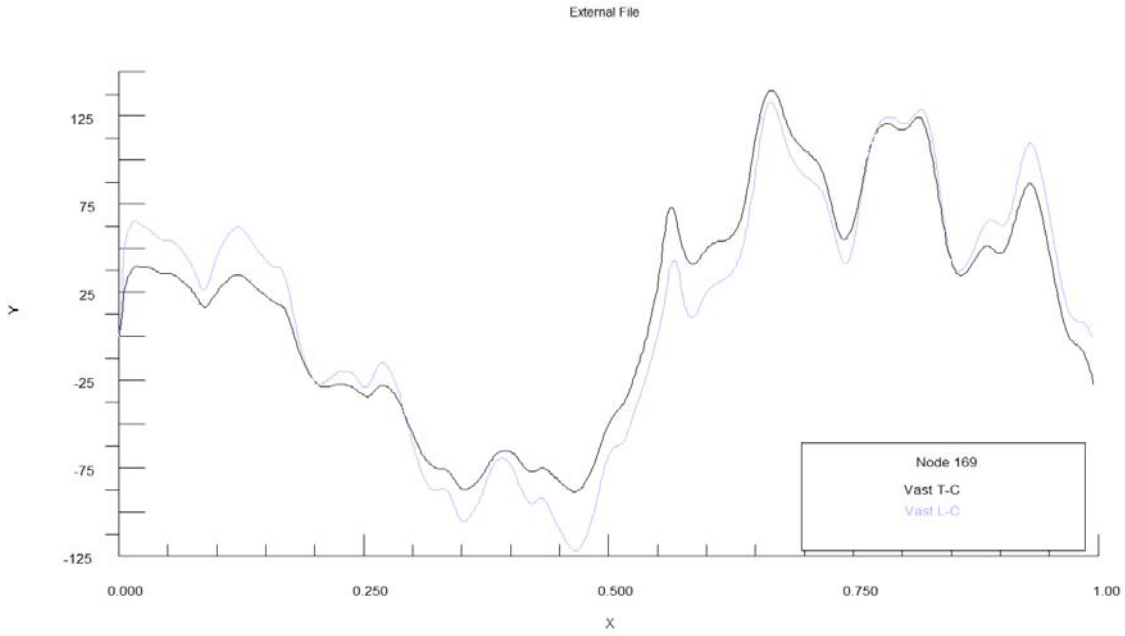

Figure 2.4.8: T-C and L-C Velocity Comparison for Node 169 - Pinned

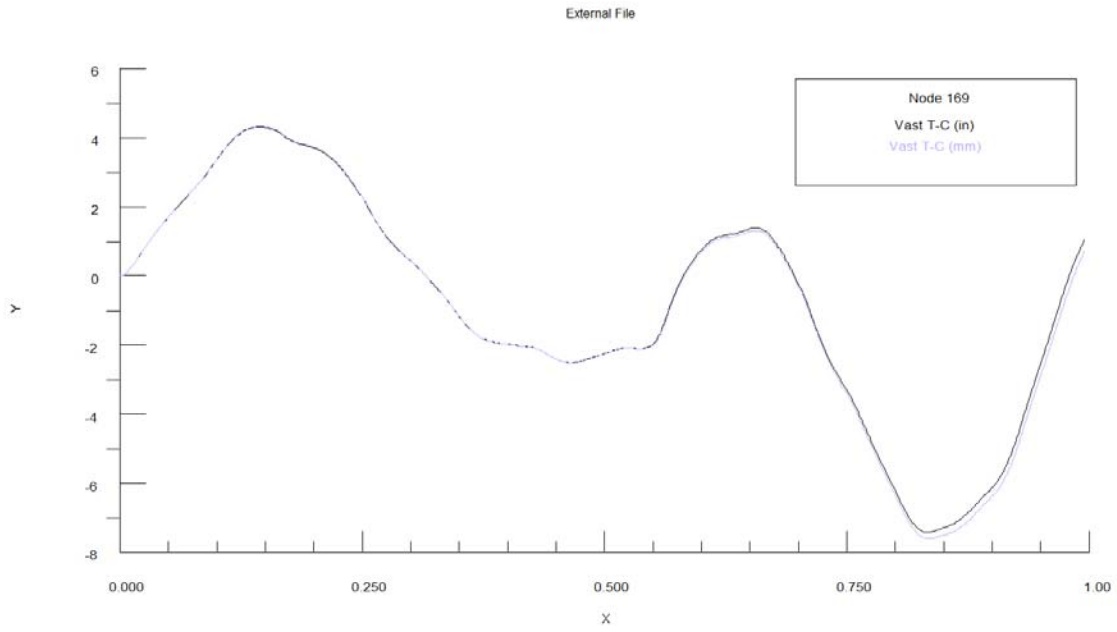

Figure 2.4.9: Displacement Comparison for Node 169 - English Units Versus Metric Units

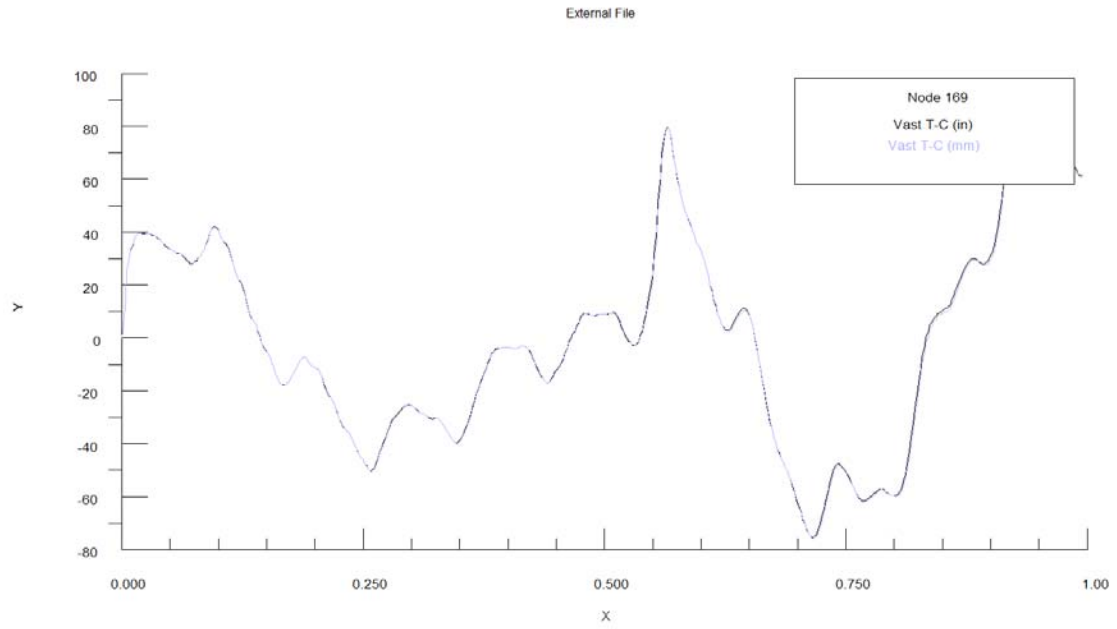

Figure 2.4.10: Velocity Comparison for Node 169 - English Units Versus Metric Units

2.5 CPF Analysis

The finite element model for the CPF is shown in Figures 2.5.1 to 2.5.3. The CPF analyses have been performed using both a doubly asymptotic approximation (DAA1) to a spherical shock wave loading and a virtual mass approximation (VMA) to a bubble pulse loading. The magnitude of the loadings is such that the vessel responds in a linear manner. Two types of boundary conditions were considered – unconstrained and pinned.

Computed displacement and velocity time histories for the unconstrained condition, for node 3920, using both the tightly-coupled (T-C) and loosely-coupled (L-C) USA interfaces, are shown in Figures 2.5.4 to 2.5.5, for the bubble loading, and Figures 2.5.6 and 2.5.7 for the shock loading..

Computed displacement and velocity time histories for the pinned condition, for node 3920, using both the tightly-coupled (T-C) and loosely-coupled (L-C) USA interfaces, are shown in Figures 2.5.8 to 2.5.9, for the bubble loading, and Figures 2.5.10 and 2.5.11 for the shock loading.

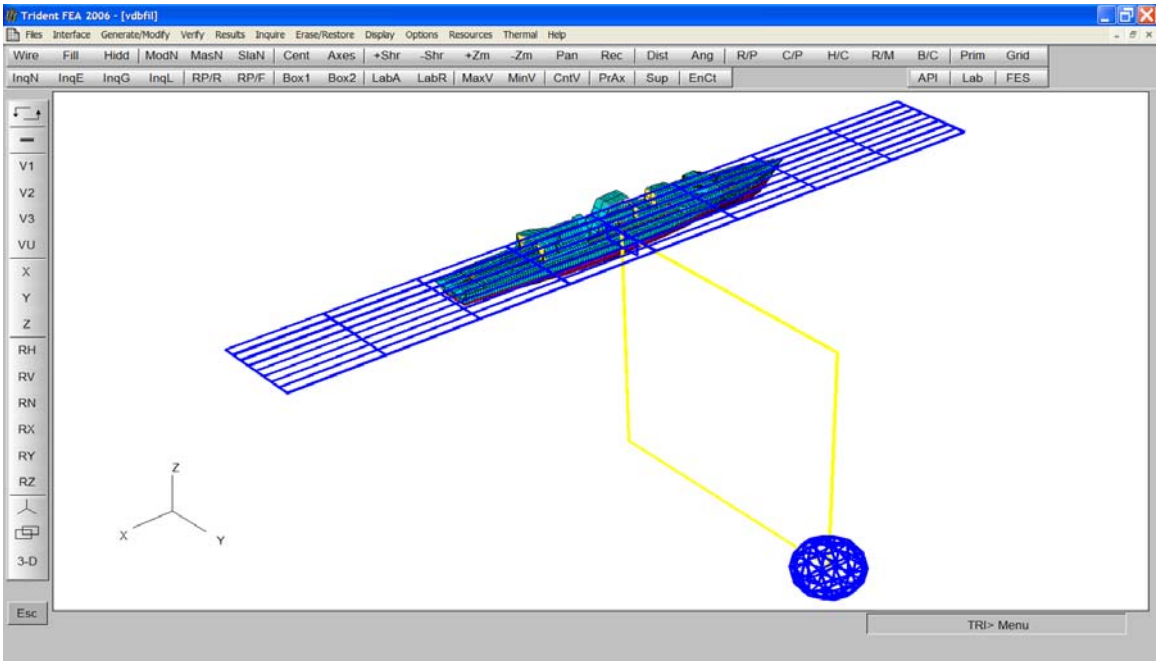

Figure 2.5.1: Trident Finite Element Model of the CPF

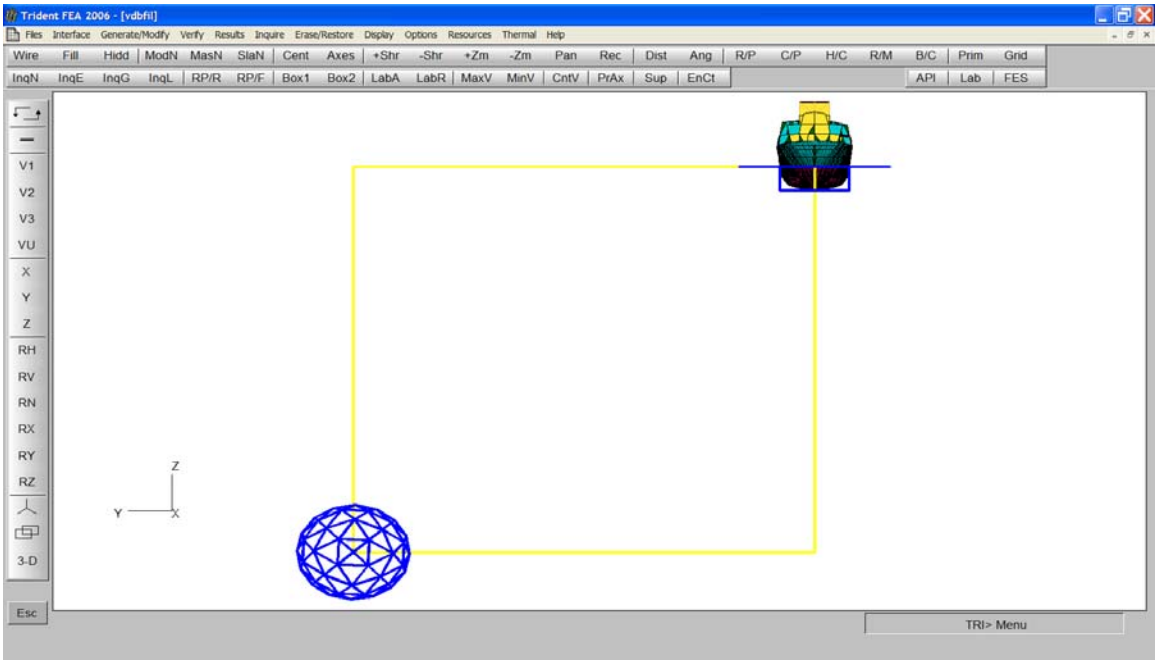

Figure 2.5.2: Trident Finite Element Model of the CPF - End View

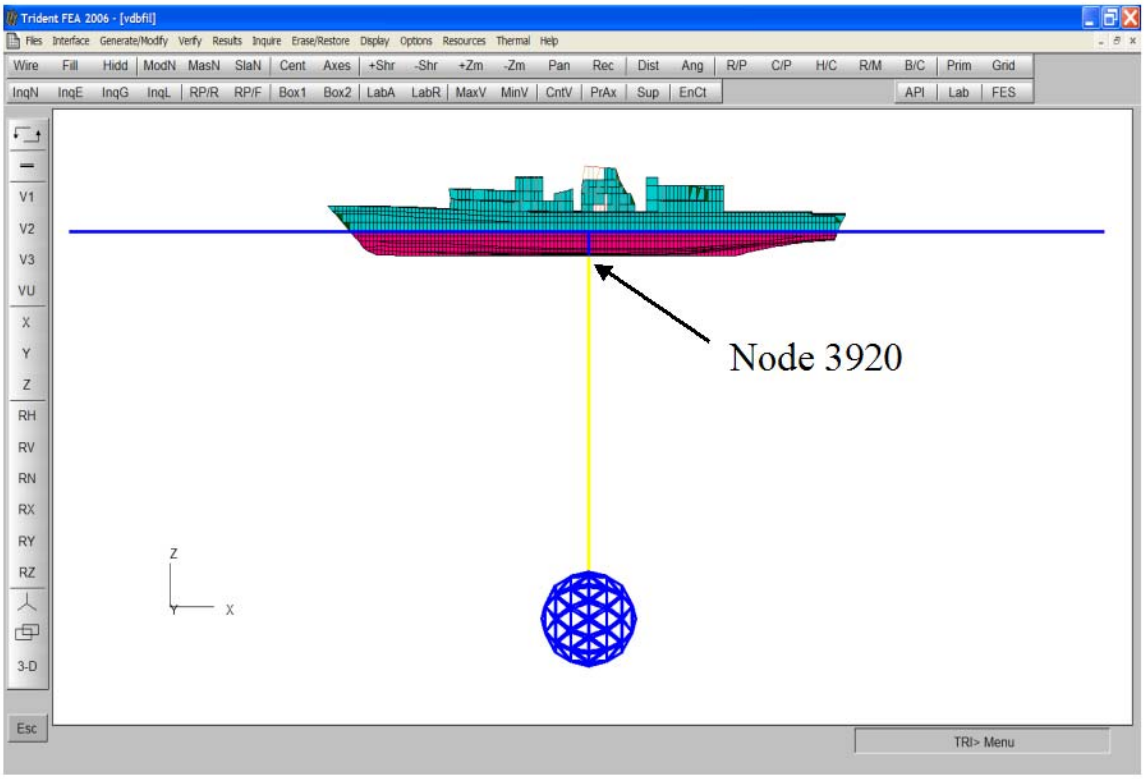

Figure 2.5.3: Trident Finite Element Model of the CPF - Side View

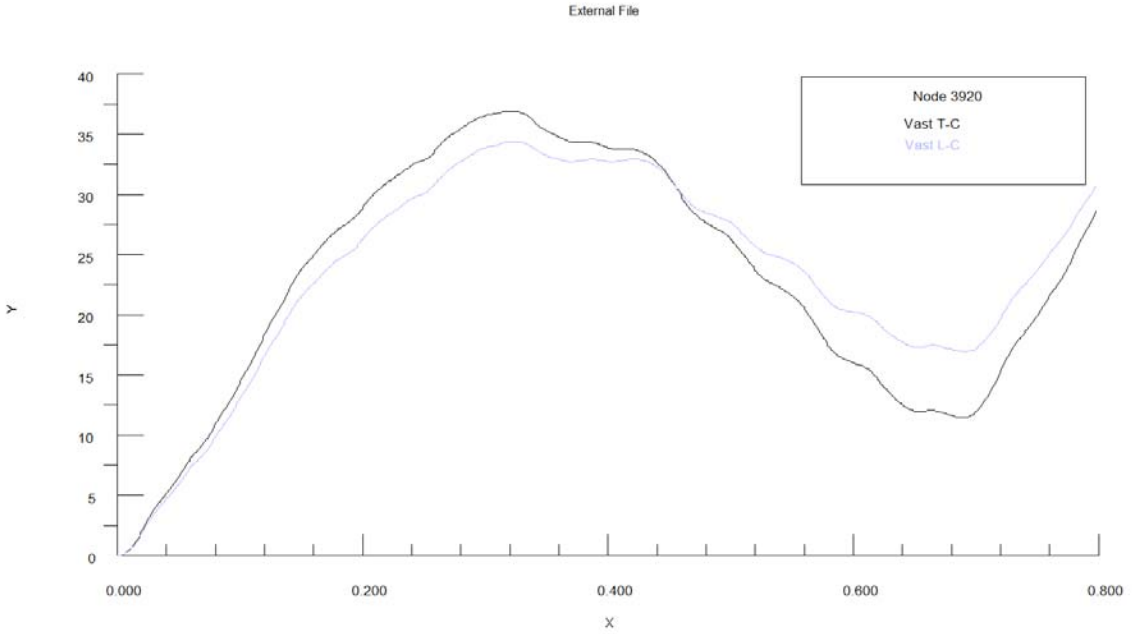

Figure 2.5.4: T-C and L-C Displacement Comparison at Node 3920 - Bubble Loading

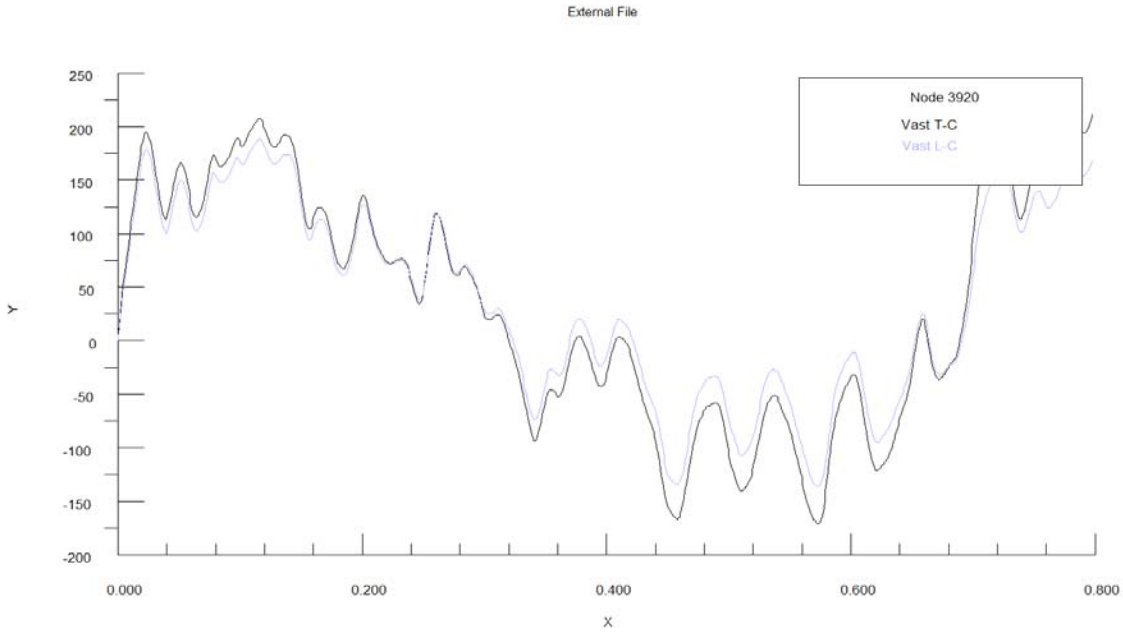

Figure 2.5.5: T-C and L-C Velocity Comparison at Node 3920 - Bubble Loading

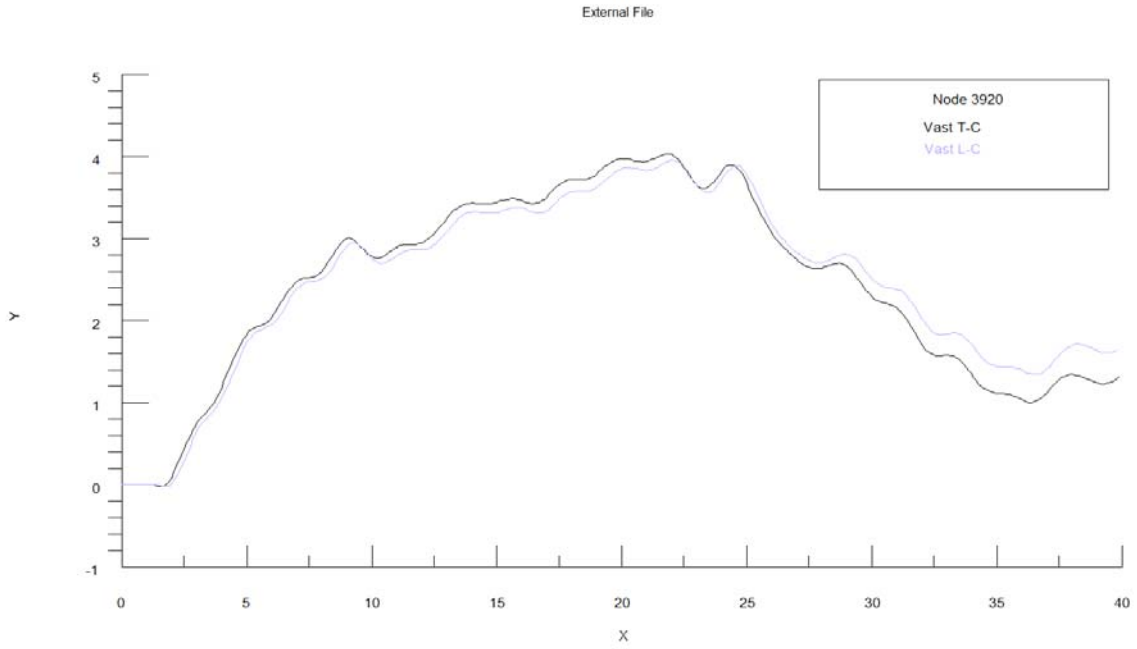

Figure 2.5.6: T-C and L-C Displacement Comparison at Node 3920 - Shock Loading

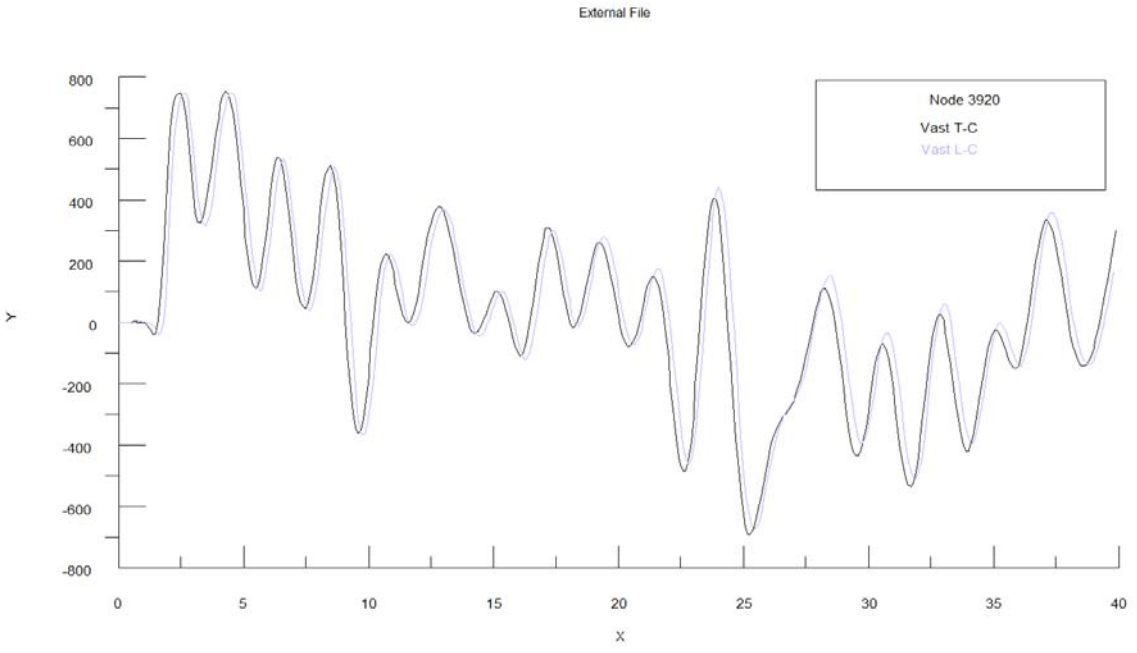

Figure 2.5.7: T-C and L-C Velocity Comparison at Node 3920 - Shock Loading

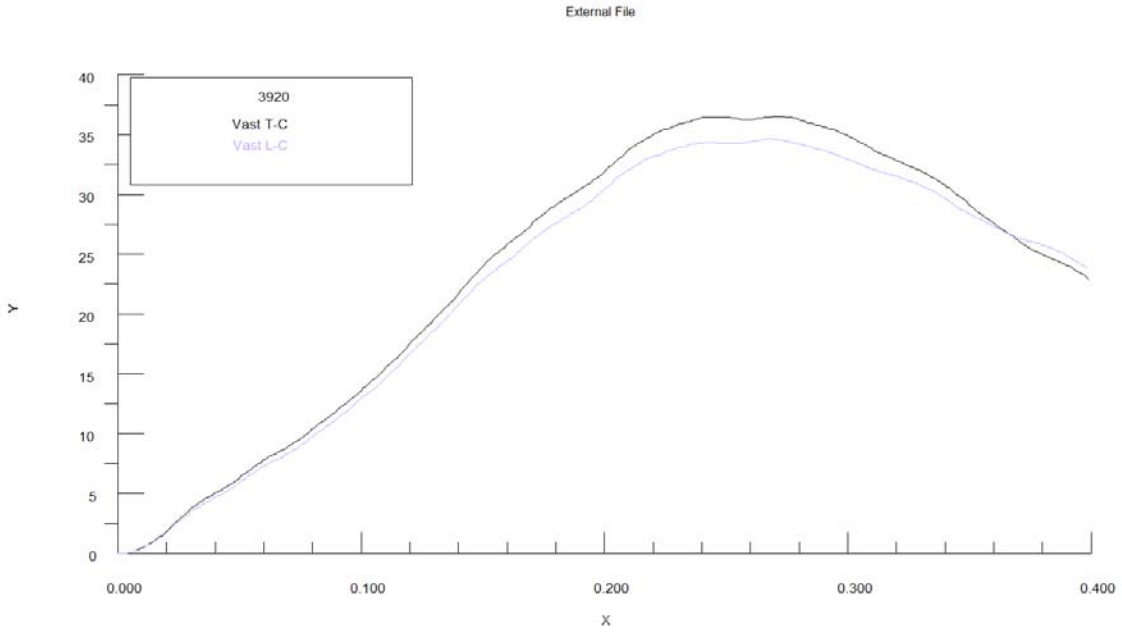

Figure 2.5.8: T-C and L-C Displacement Comparison at Node 3920 - Bubble Loading - Pinned

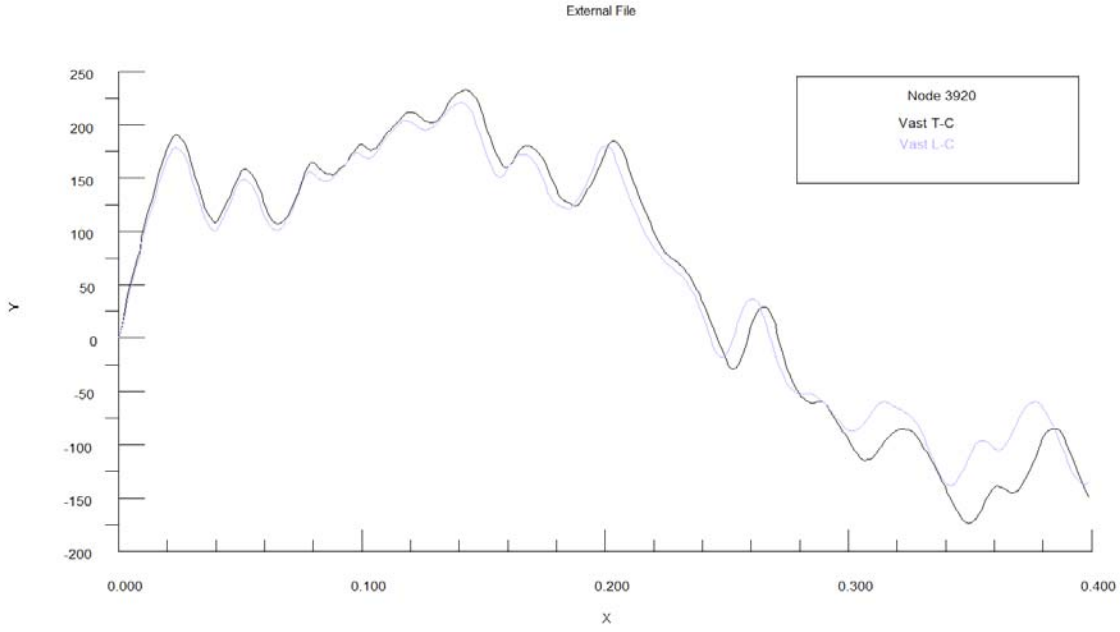

Figure 2.5.9: T-C and L-C Velocity Comparison at Node 3920 - Bubble Loading - Pinned

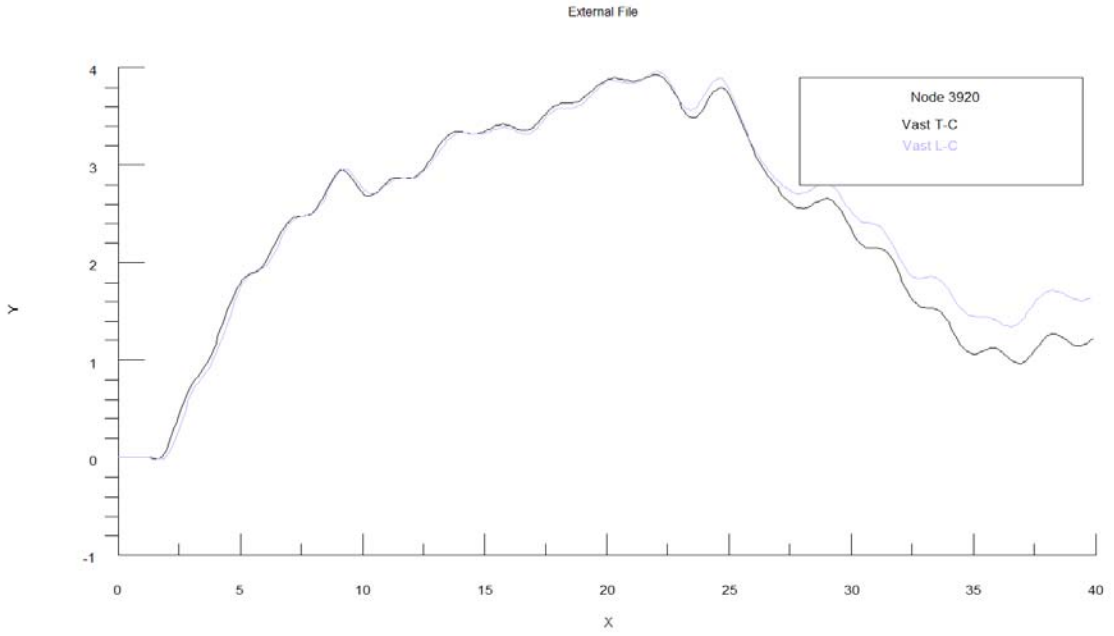

Figure 2.5.10: T-C and L-C Displacement Comparison at Node 3920 - Shock Loading - Pinned

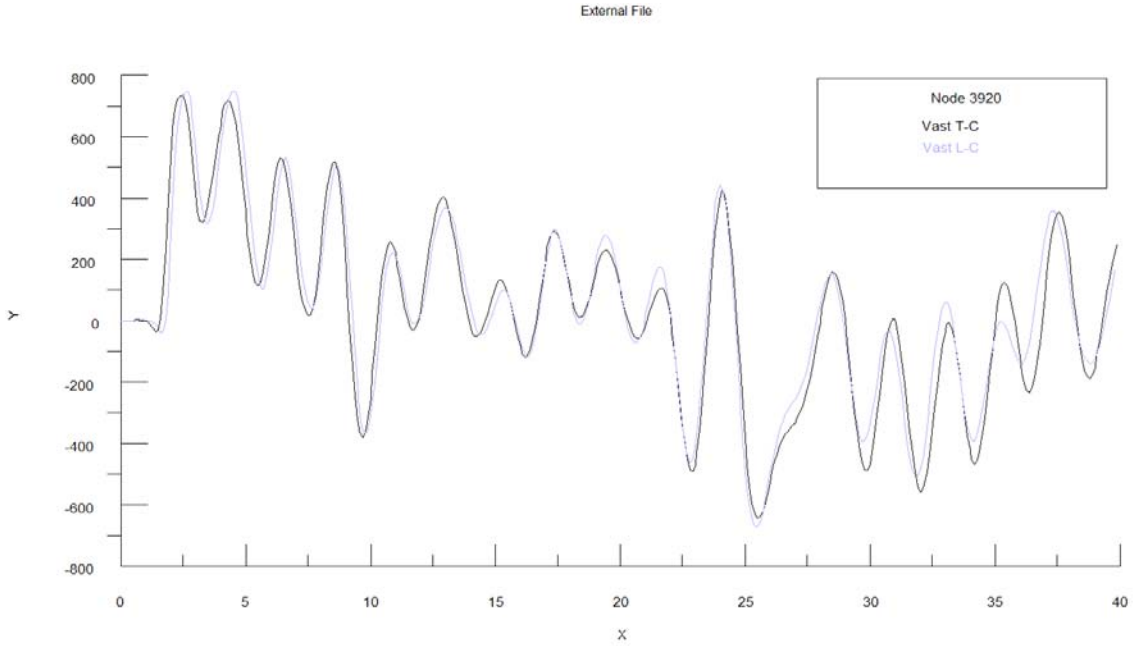

Figure 2.5.11: T-C and L-C Velocity Comparison at Node 3920 - Shock Loading - Pinned

2.6 Suffield Circular Plate Analysis

The experimental setup for the Suffield circular plate problem is shown in Figure 2.6.1. The analyses have been performed using both a doubly asymptotic approximation (DAA1) to a spherical shock wave loading and a virtual mass approximation (VMA) to a bubble pulse loading. The magnitudes of the loadings are such that the plate responds both linearly and nonlinearly.

The finite element model for the full model is shown in Figure 2.6.2. The finite element model making use of quarter symmetry is shown in Figure 2.6.3. The results presented here are for the quarter symmetry model. All USA analyses were performed using the new tightly-coupled interface.

A typical charge configuration is shown in Figure 2.6.4. Two charge scenarios were considered: (1) Shot 1 – weight = 100g C4 (127 g TNT equivalent), standoff = 7.5 ft., depth = 13.5; and (2) Shot2 – weight = 250 g C4 (305 g TNT equivalent), standoff = 4.5 ft., depth = 16.5. The water surface was taken to be 21.0 ft. above the target panel.

The displacement time history comparisons for USA versus experiment for the shot 1 and 2 shock loading cases for linear analysis with no damping are shown in Figures 2.6.5 and 2.6.6.

The displacement time history comparisons for USA versus experiment for the shot 1 and 2 bubble loading cases for linear analysis with no damping are shown in Figures 2.6.7 and 2.6.8.

The displacement time history comparisons for USA versus experiment for the shot 1 and 2 bubble loading cases for linear analysis with damping (ADAMP = 200.0 and BDAMP = 0.0) are shown in Figures 2.6.9 and 2.6.10.

The displacement time history comparisons for USA linear analysis versus nonlinear analysis for the shot 1 and 2 bubble loading cases with no damping are shown in Figures 2.6.11 and 2.6.12.

The displacement time history comparisons for USA nonlinear analysis versus experiment for the shot 1 and 2 bubble loading cases with no damping are shown in Figures 2.6.13 and 2.6.14. The material properties used in the analyses were as follows: Young’s Modulus = 207000.0; Poisson’s Ratio = 0.3; Initial Yield Stress = 550.0; Isotropic Tangent Modulus = 0.0; and Kinematic Tangent Modulus = 2000.0. Both geometric and material nonlinearities were included.

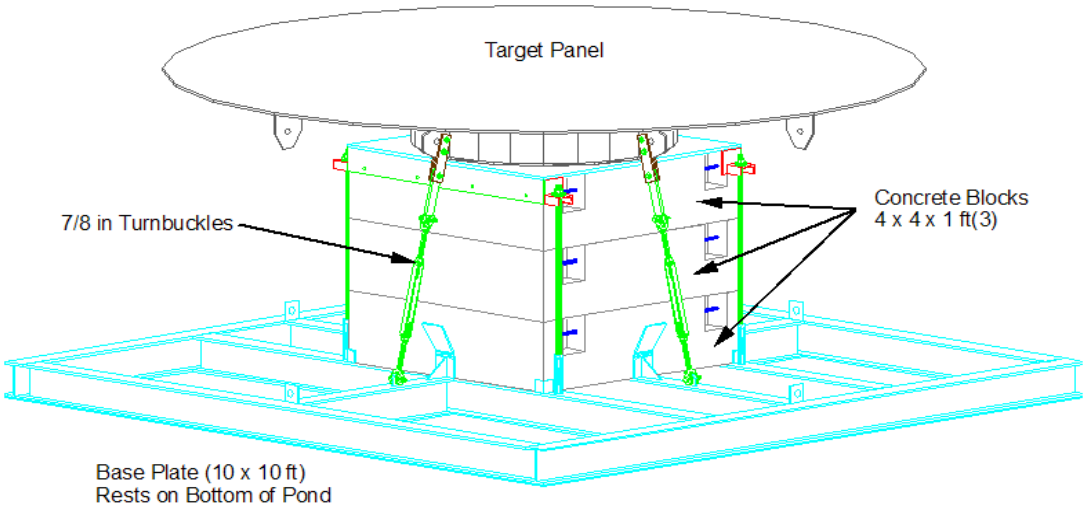

Figure 2.6.1: Circular Plate Experimental Setup

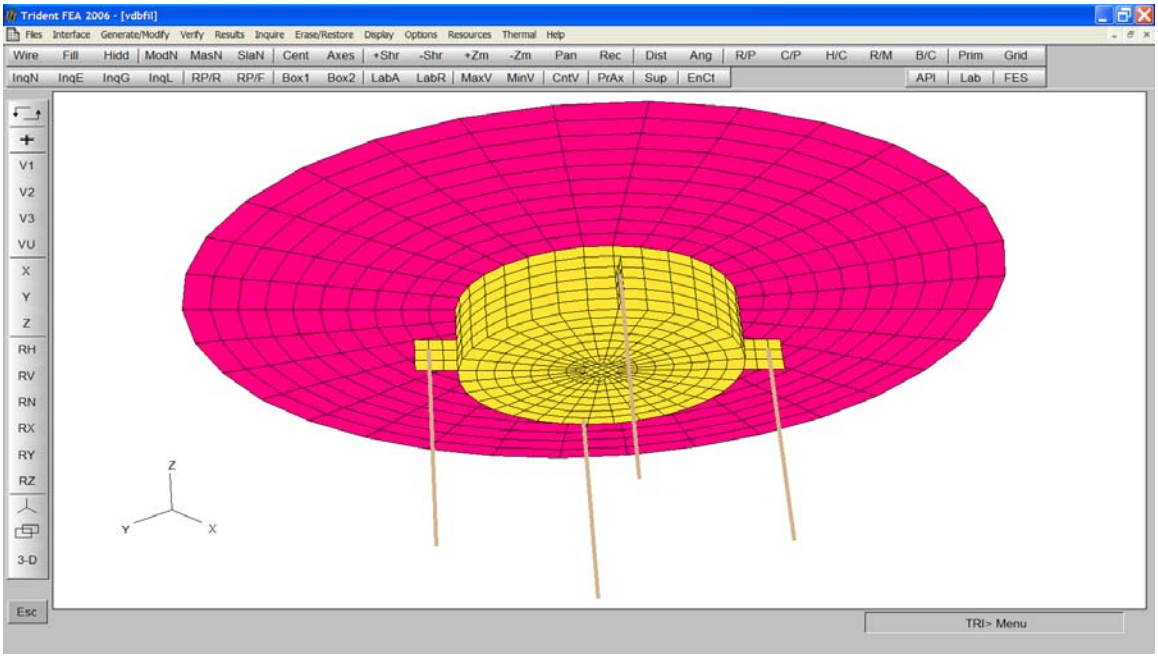

Figure 2.6.2: Trident Finite Element Model of Circular Plate

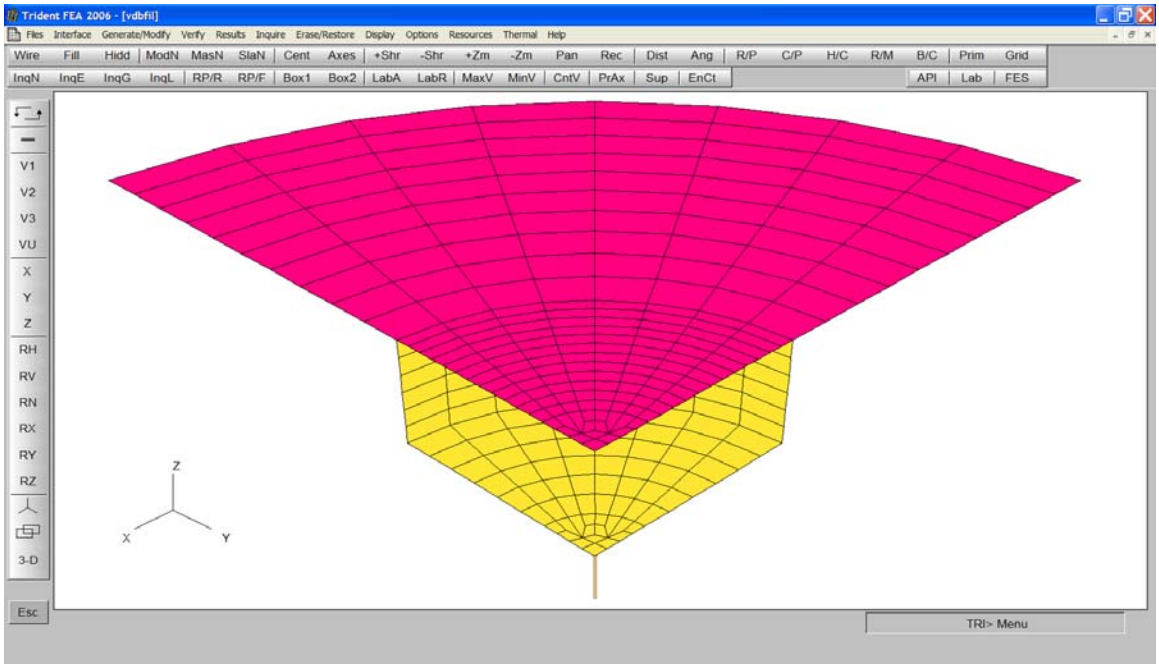

Figure 2.6.3: Trident Finite Element Quarter Model of Circular Plate

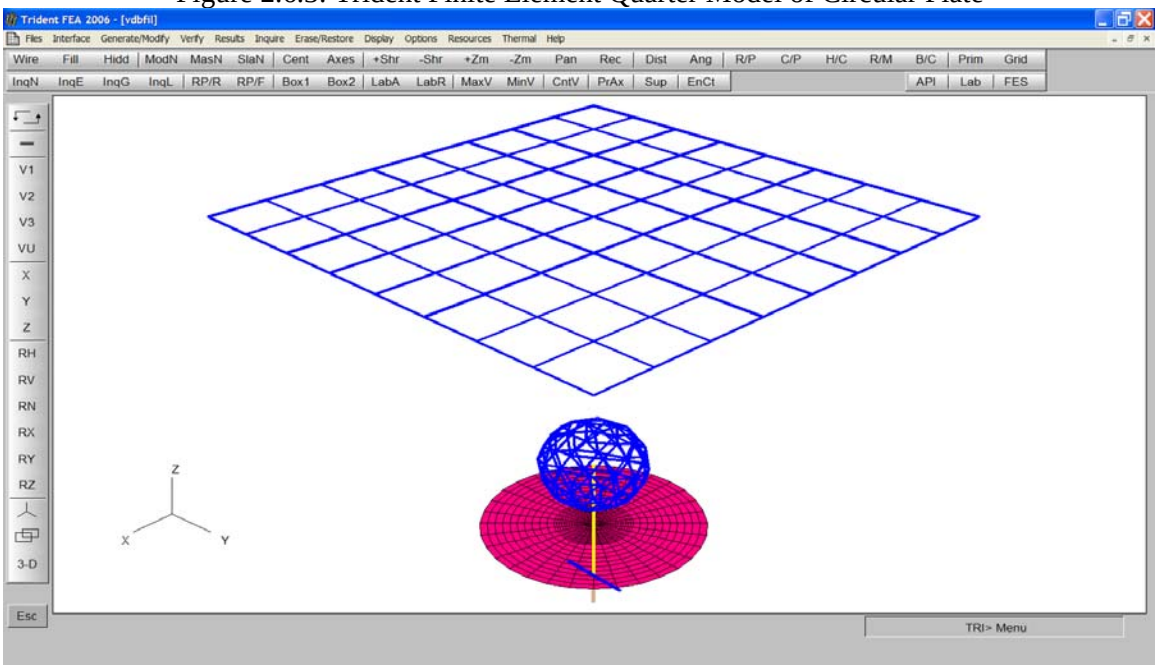

Figure 2.6.4: Typical Charge Configuration for Circular Plate

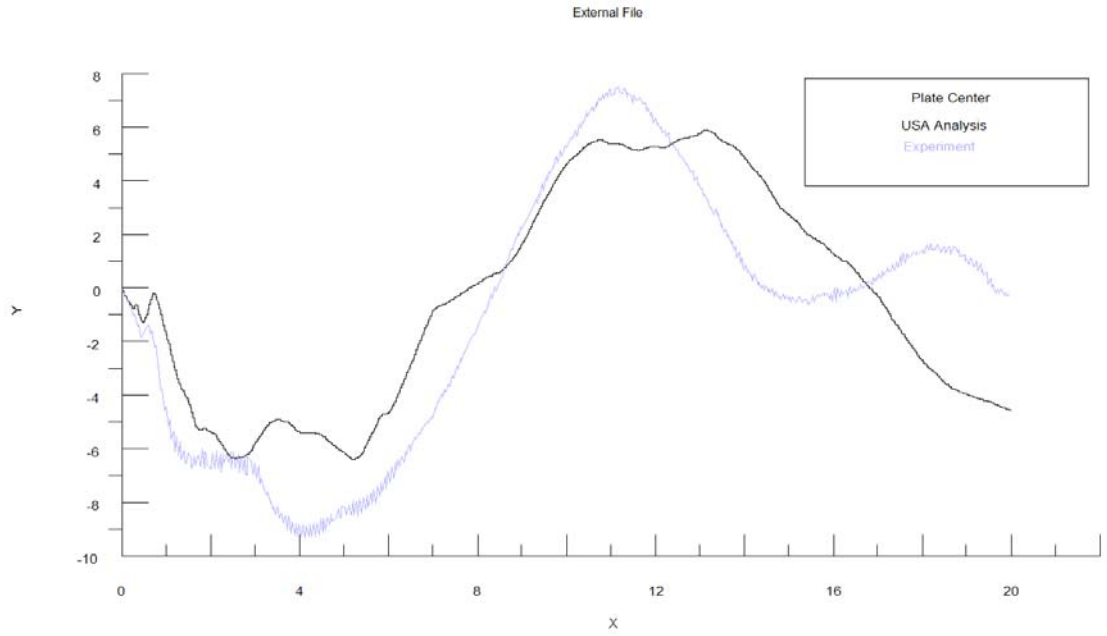

Figure 2.6.5: USA Linear Analysis Versus Experiment - Center Plate Displacement - Shot 1 Shock Loading

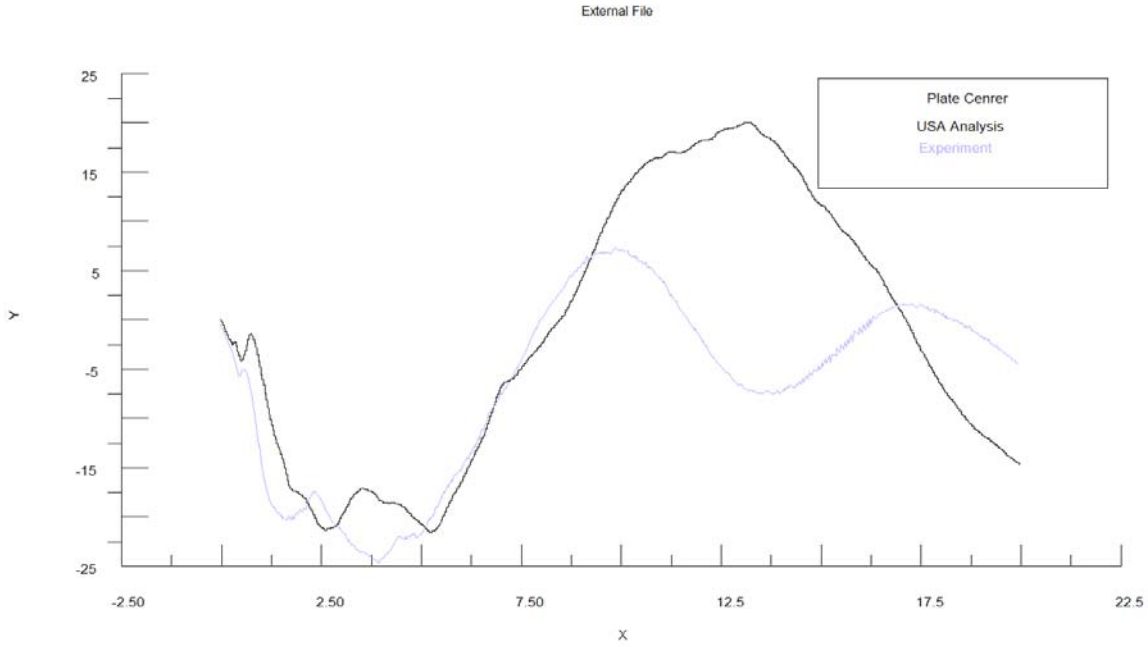

Figure 2.6.6: USA Linear Analysis Versus Experiment - Center Plate Displacement - Shot 2 Shock Loading

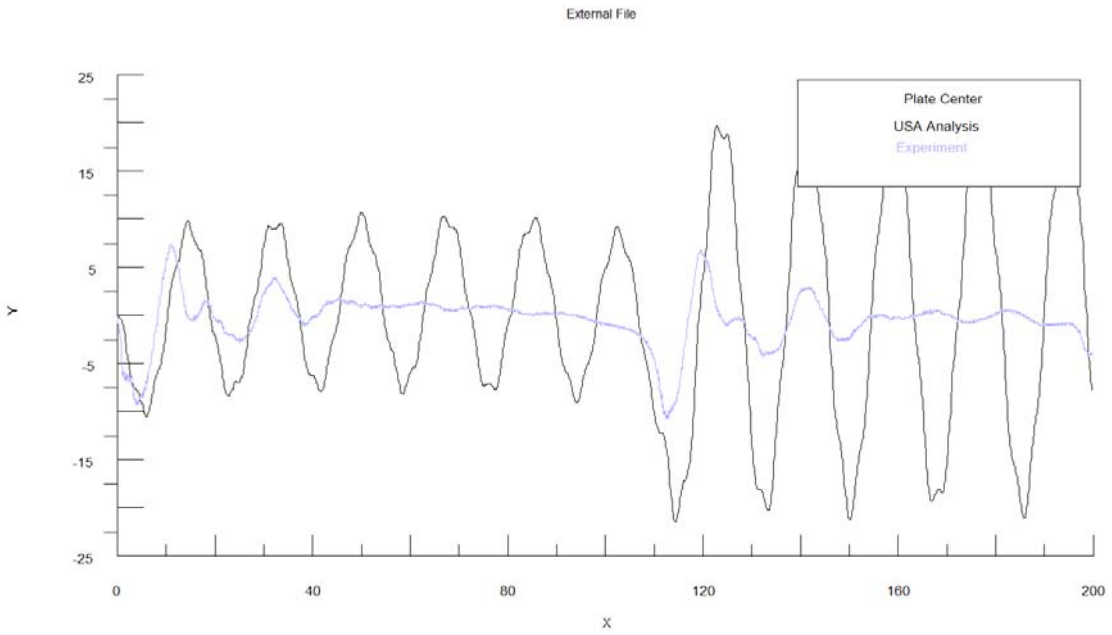

Figure 2.6.7: USA Linear Analysis Versus Experiment - Center Plate Displacement - Shot 1 Bubble Loading

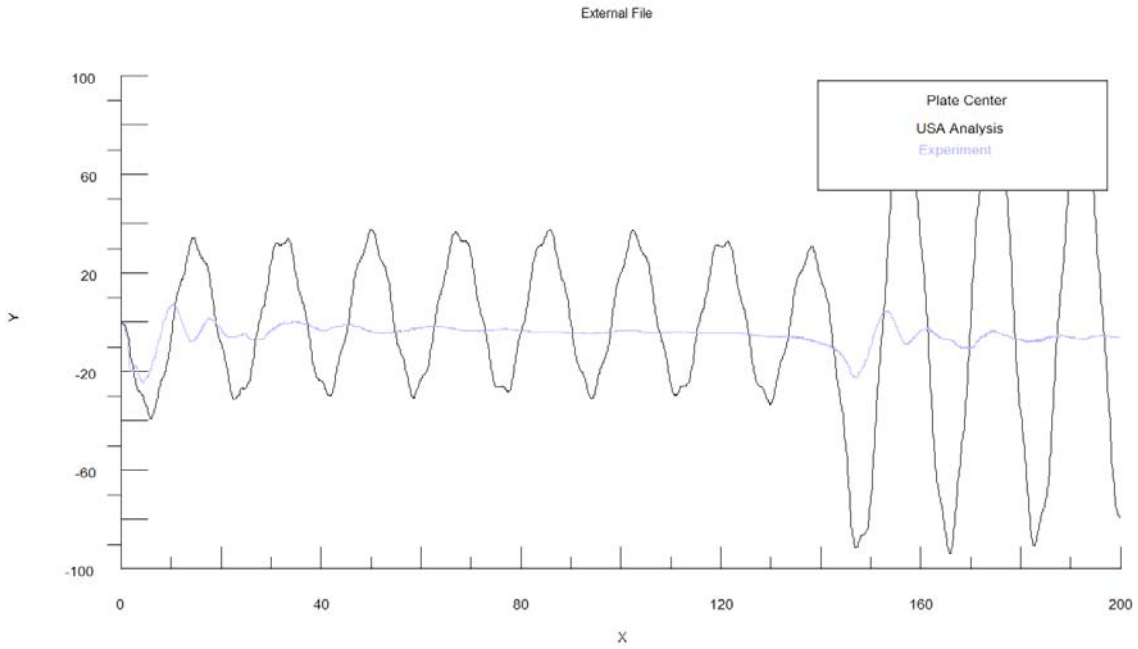

Figure 2.6.8: USA Linear Analysis Versus Experiment - Center Plate Displacement - Shot 2 Bubble Loading

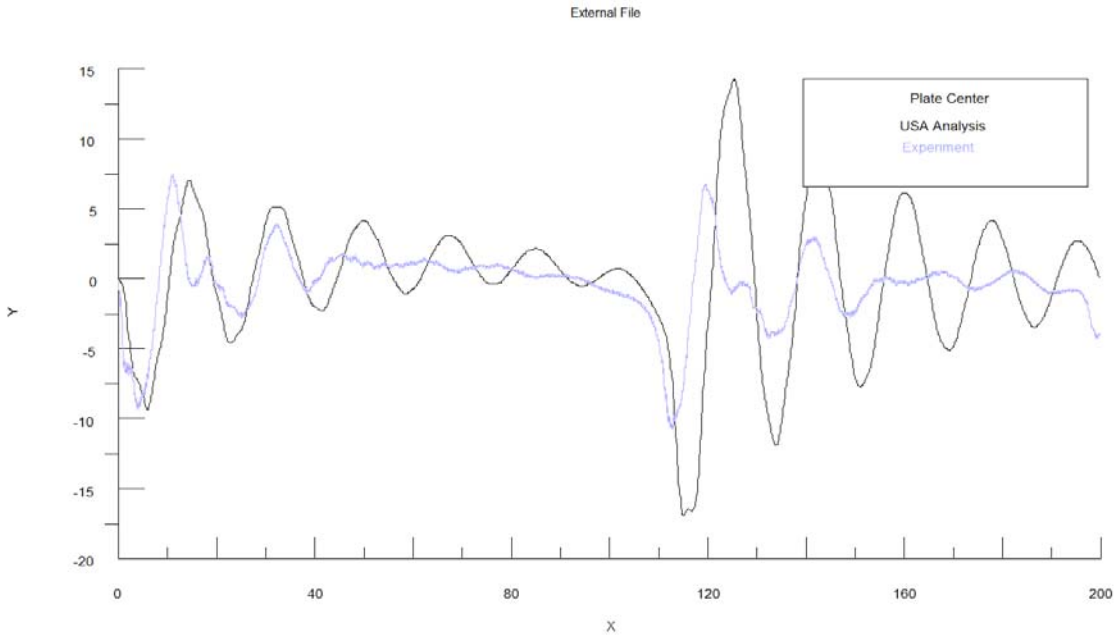

Figure 2.6.9: USA Linear Analysis with Damping Versus Experiment - Center Plate Displacement - Shot 1 Bubble Loading

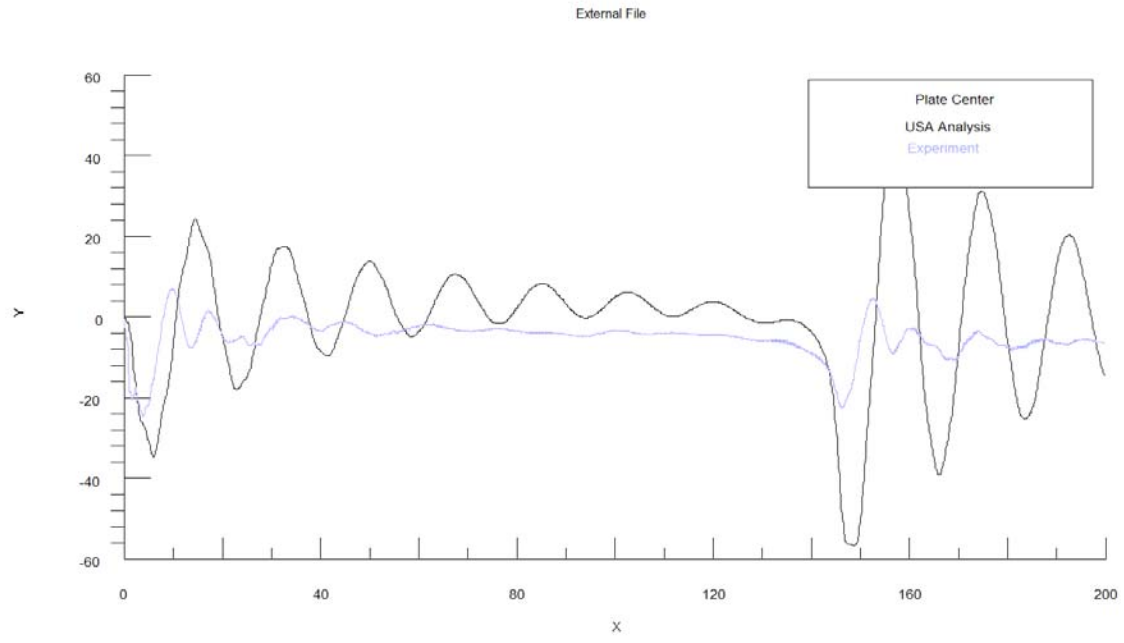

Figure 2.6.10: USA Linear Analysis with Damping Versus Experiment - Center Plate Displacement - Shot 2 Bubble Loading

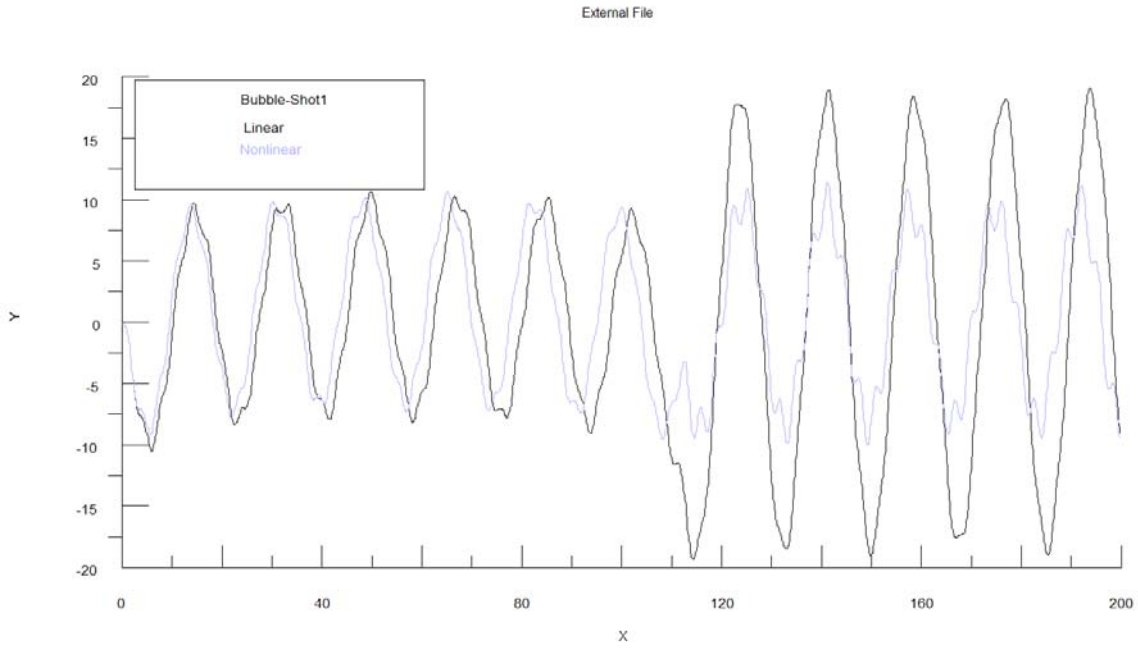

Figure 2.6.11: USA Linear Analysis Versus Nonlinear Analysis - Center Plate Displacement - Shot 1 Bubble Loading

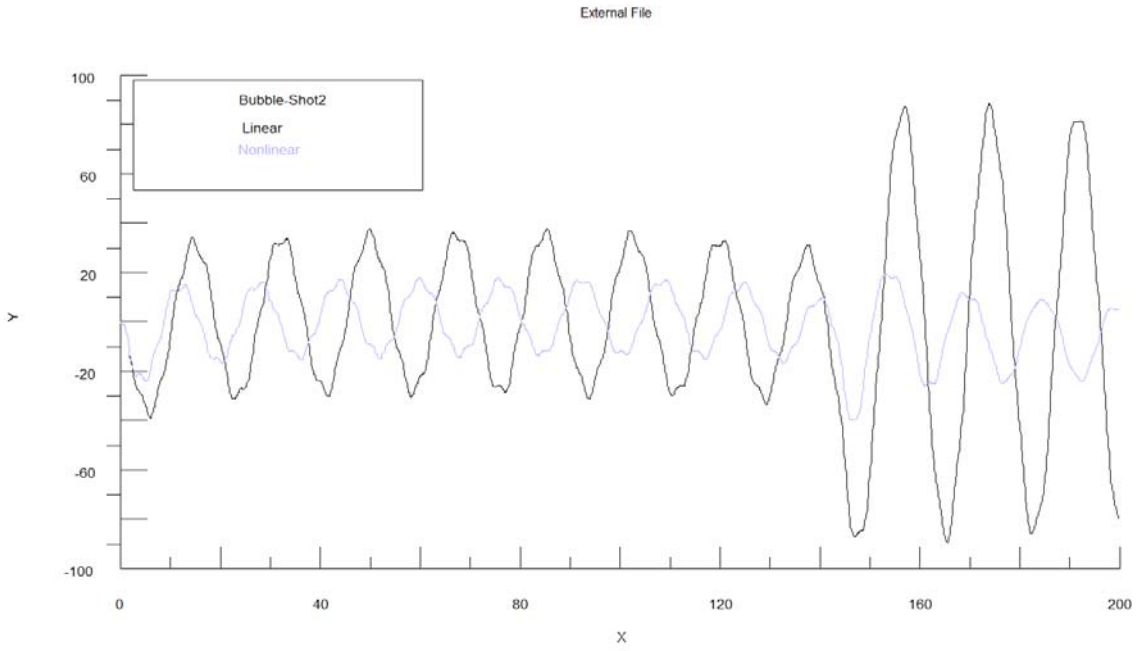

Figure 2.6.12: USA Linear Analysis Versus Nonlinear Analysis - Center Plate Displacement - Shot 2 Bubble Loading

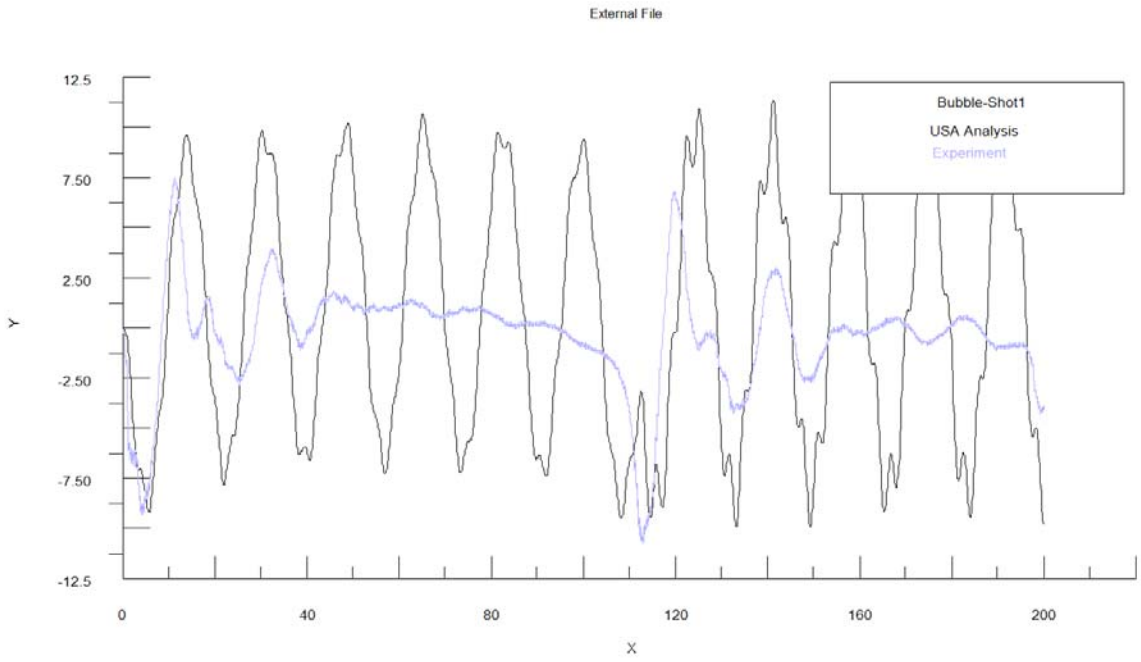

Figure 2.6.13: USA Nonlinear Analysis Versus Experiment - Center Plate Displacement - Shot 1 Bubble Loading

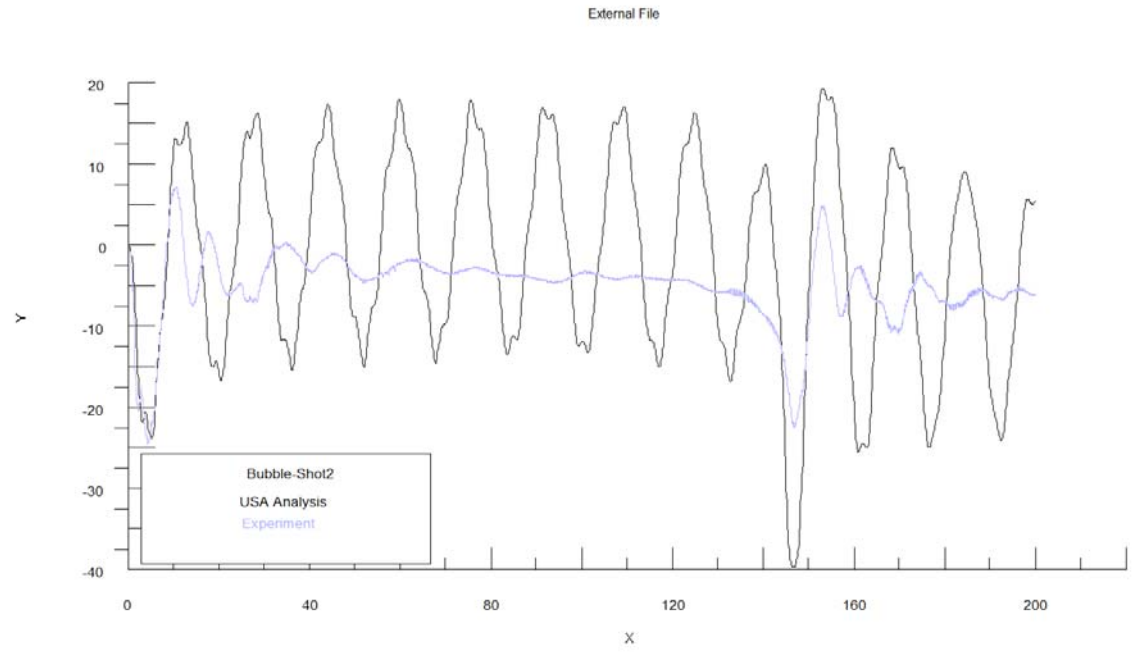

Figure 2.6.14: USA Nonlinear Analysis Versus Experiment - Center Plate Displacement - Shot 2 Bubble Loading

3. Automatically Generating Input Files for USA Analysis

In the case of loosely-coupled USA analysis, there are five data sets required, one for each of the modules VASUSA, FLUMAS, AUGMAT, TIMINT and USAVAS. For closely-coupled analysis, there are four data sets, one for each of the modules VASUSA, FLUMAS, AUGMAT and TIMINT.

In the Trident-USA interface, the following file naming convention is used: *prefix*vut.inp, *prefix*vut.out, *prefix*flu.inp, *prefix*flu.out, *prefix*tim.inp, *prefix*tim.out, *prefix*uvt.inp and *prefix*uvt.out. Here "*prefix*" is a user defined file name prefix. The extension "inp" refers to input file required by the module and "out" refers to the output file created by the module.

The new USA interface allows for the automatic generation of the all four data sets, in a single step, when using the tightly-coupled link. When using the loosely-coupled link, only the data sets for modules VASUSA and USAVAS can be automatically generated.

The files automatically generated for the modules FLUMAS, AUGMAT and TIMINT are in the keyword format only. When providing the necessary input parameters, the user has the option to apply data stored on a UNDEX charge data file.

The USA interface dialogues for generating the files *prefix*vut.inp, *prefix*flu.inp, *prefix*aug.inp and *prefix*tim.inp for tightly-coupled analyses are shown in Figure 3.1.

The USA interface dialogues for generating the *prefix*vut.inp and *prefix*uvt.inp for loosely-coupled analyses are shown in Figure 3.2.

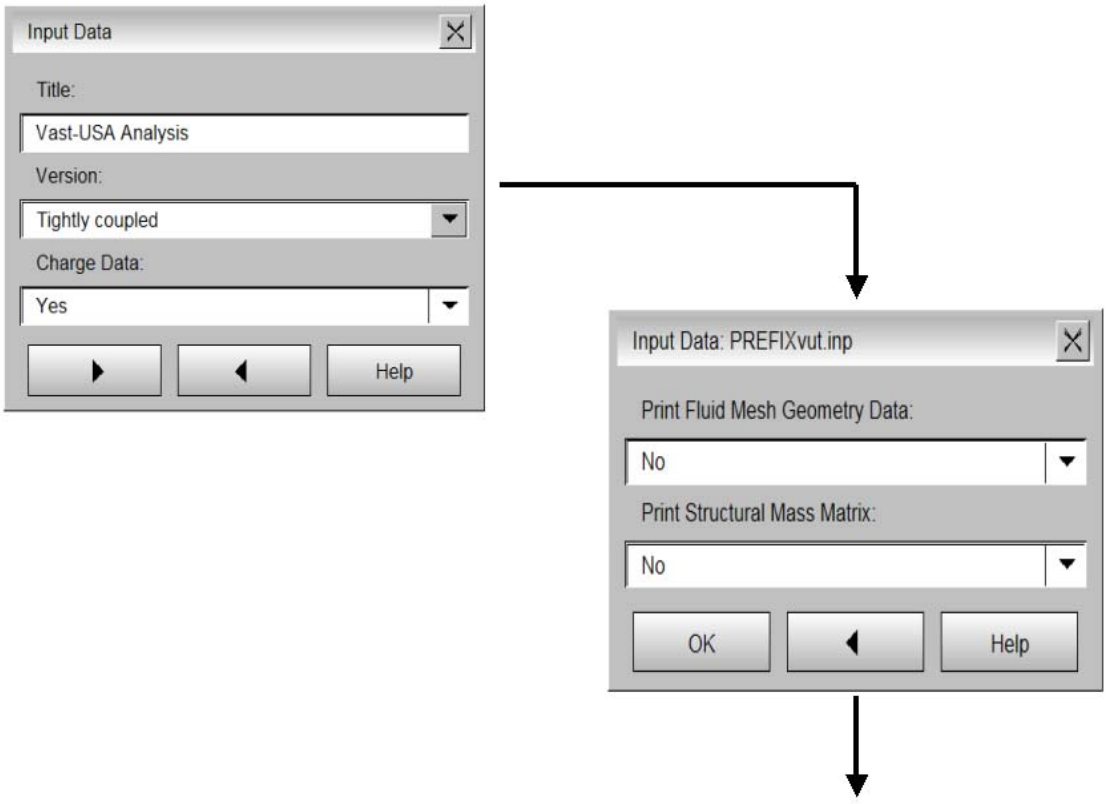

Figure 3.1: USA Interface Dialogues for generating Input Files for Tightly-coupled Analysis

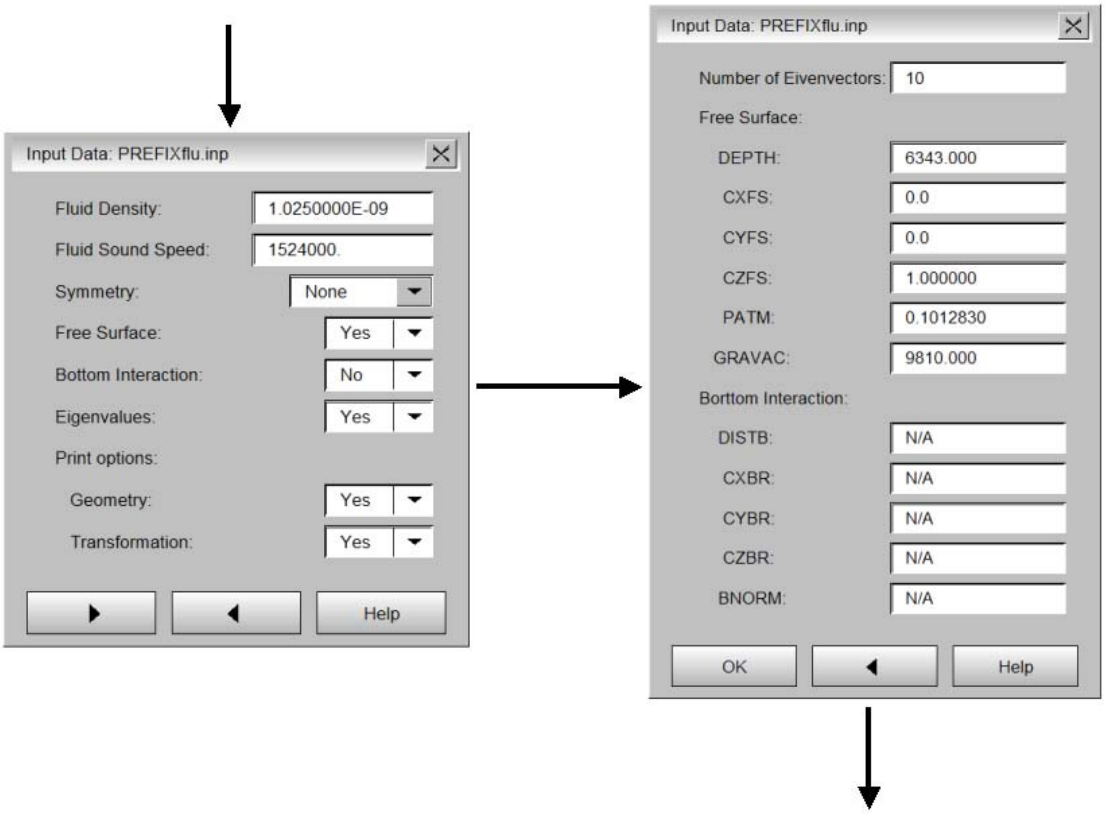

Figure 3.1: USA Interface Dialogues for generating Input Files for Tightly-coupled Analysis (cont'd)

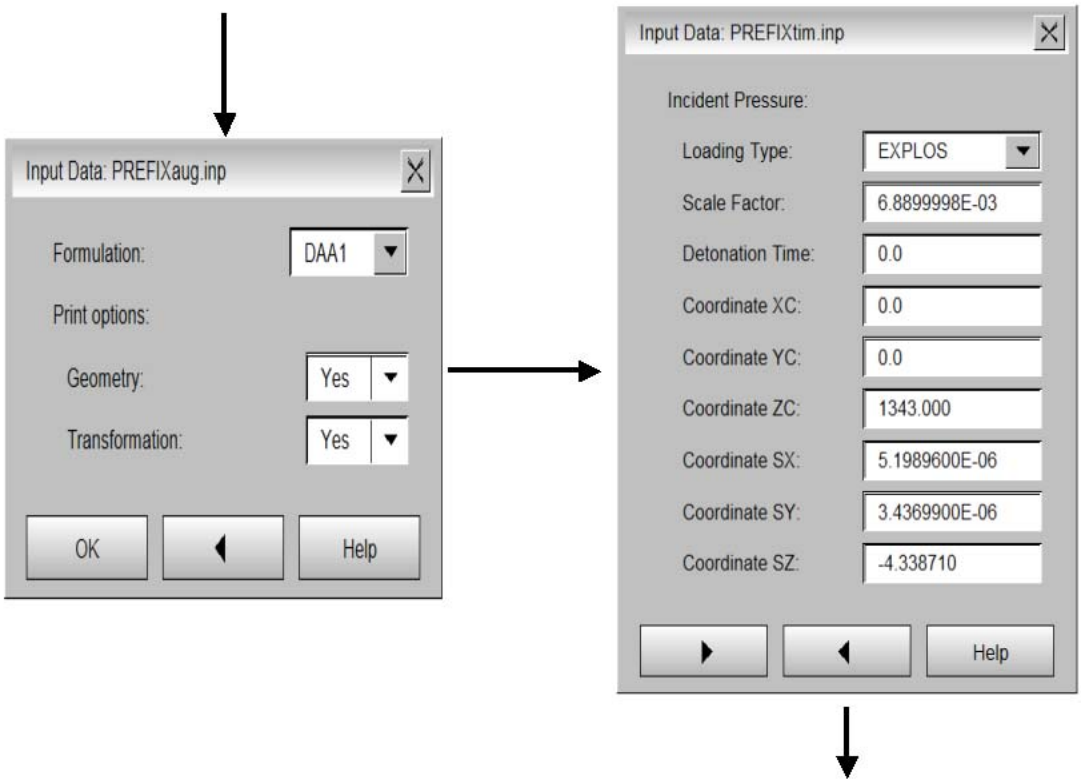

Figure 3.1: USA Interface Dialogues for generating Input Files for Tightly-coupled Analysis (cont'd)

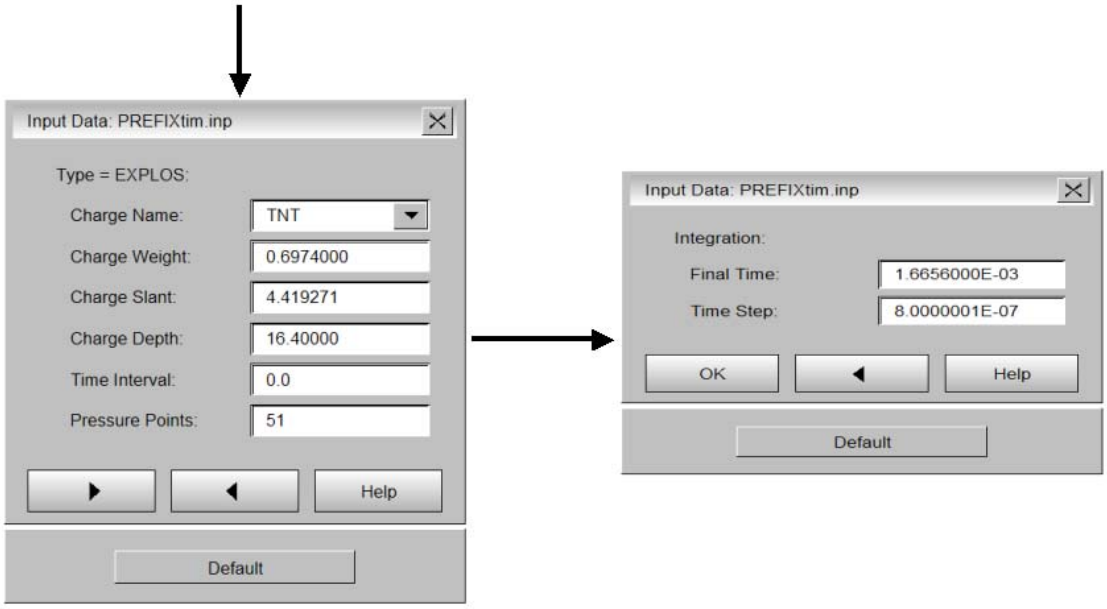

Figure 3.1: USA Interface Dialogues for generating Input Files for Tightly-coupled Analysis (cont'd)

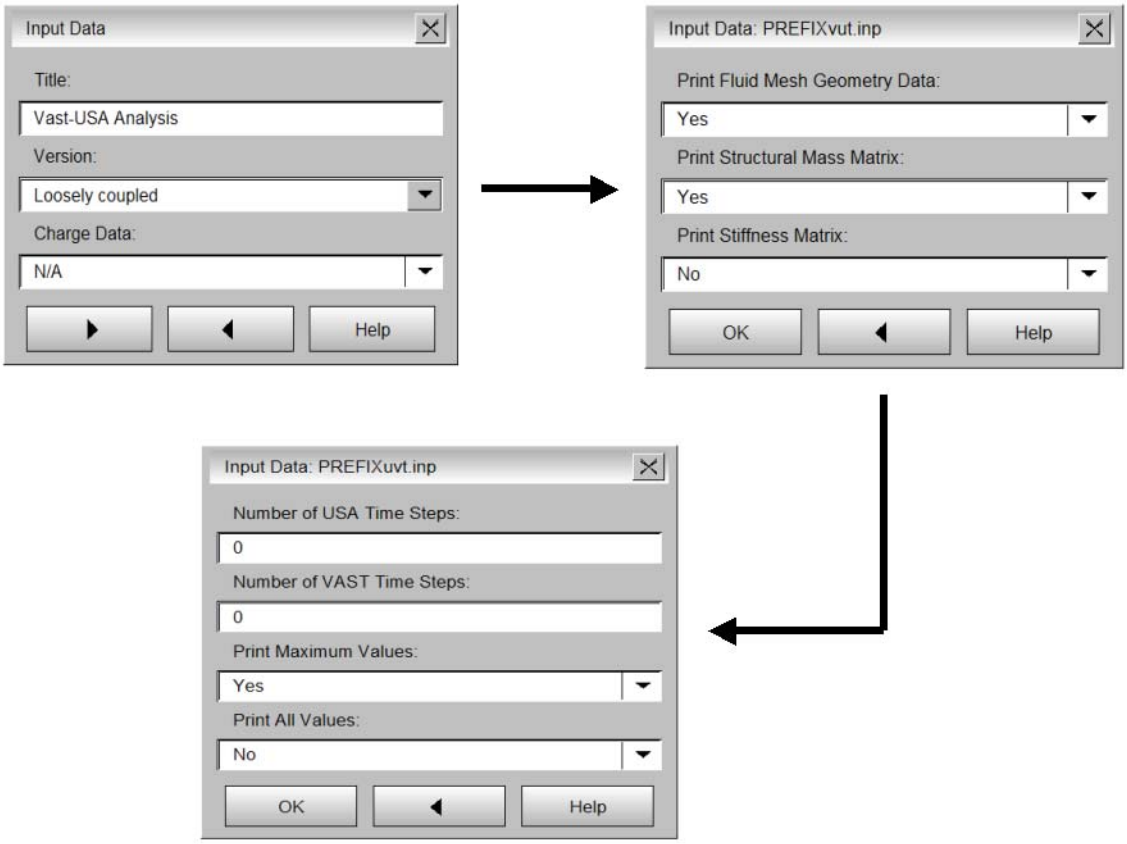

Figure 3.2: USA Interface Dialogues for generating Input Files for Loosely-coupled Analysis

4. Literature Review of BEM Techniques for Underwater Explosion Modeling

4.1 Introduction

Underwater explosion cavities have been the subject of considerable study. Although reasonable numerical models have been developed to approximate cavities in the far field for infinite and semi-infinite domains as well as simple geometries, there has been less success in developing a more general, near-field solution. This is partly due to the complexity of modeling the involved phenomena; cavities migrate, undergo expansion/contraction cycles, merge and depending on the specific case, form jets that strike nearby boundaries. In spite of (or perhaps because of) this complexity, cavitation dynamics has seen active research for a number of decades aimed at improving the understanding of the phenomena, since bubble formation and collapse has important military, industrial, and biomedical applications.

This section describes a literature review into boundary element techniques for near-field UNDEX simulation. Boundary element techniques lie in the middle of techniques for UNDEX simulations in terms of physical representation and computation time. The rest of the introduction discusses the three main techniques used to model UNDEX cavities in order to put boundary elements methods in context, while the remainder of this review focuses on boundary element methods, including their theoretical basis, limitations, and implementation details.

There are essentially three separate categories of models that have been developed to handle UNDEX cavities. The first category is simplified models [Wardlaw 1998] and [Moyer 2003] that attempt to reproduce the effects of an UNDEX cavity through a highly simplified representation. These methods, although computationally efficient, are effectively limited to far-field cases where the influence of the geometry of the fluid domain on the bubble itself is negligible.

The other two categories have seen increased interest in the past three decades due to their applicability to near-field cases where the geometry of the boundary plays a significant role in the behavior of the cavity. These categories are Computational Fluid Dynamics (CFD) and Boundary Element Methods (BEMs).

CFD approaches are the most general of the two and come in varying degrees of complexity, but for the simulation of UNDEX cavities multi-material Eulerian solvers are most common (e.g. LS-DYNA, AutoDYN, Chinook). These solvers work by discretizing the fluid volume, and then applying finite-difference, finite-volume or finite-element techniques to integrate the governing partial differential equations forward in time. One of the advantages of using an Eulerian CFD approach is that acoustic wave transmission (e.g. shock wave from an underwater charge and bubble pulses) is included in the model by default. Furthermore, CFD approaches can be arbitrarily complicated, including everything from heat/mass transfer to viscosity and turbulence. However CFD approaches require significant computational resources and suffer from a number of numerical defects such as smearing the cavity interface, instabilities due to fluid mixing, numerical diffusion of shocks and poor efficiency. The poor efficiency is often due to the compressible (wave-transmission) portions of the simulation occupying only a very small fraction of the total runtime, since the acoustic timescales are on the order of milliseconds or less, while the bubble timescales are on the order of tenths of seconds to seconds. Consequently a large portion of the simulation runtime is spent simulating an incompressible (not acoustic) problem

using the limitations of acoustic wave propagation schemes. Furthermore, the generality afforded by CFD approaches may be overkill for many practical applications involving cavity dynamics.

By comparison, BEM approaches (which are the primary focus of this review) simplify the physical model of the scenario to the point where the governing equations can be transformed from differential equations into integral equations. The integral equations can be solved using iterative linear system solvers, and yield (among other things) the boundary velocities. These velocities are used to advance the position of the domain boundary in time, at which point the integral equations are evaluated again, new velocities are calculated, and the process repeats until the simulation ends. BEMs have the advantage of having relatively modest memory, computation, and pre/post processing requirements, but the drawback of requiring dramatic simplifications to the governing equations in order to transform them into integral equations. They cannot, for example, handle charge detonation, acoustic wave propagation or viscosity, among other phenomena. BEMs also suffer from the additional drawback of not scaling well, since the system of equations produced is dense, resulting in an $O(N^3)$ solution time (for direct solvers), unless more sophisticated techniques such as multipole solvers are used. The suitability of BEM techniques for a given application is consequently largely problem dependent. However BEM techniques can be augmented with other methods in order to provide a more complete representation of the problem. Using an Eulerian method to handle charge detonation and shock propagation, and a BEM to handle cavity growth and collapse is one example where a hybrid method might achieve the benefits of both techniques without the drawbacks of either.

This section details the results of a literature review of Boundary Element Methods as applied to UNDEX cavity simulation.

4.2 UNDEX Cavity BEM Overview

Review of a number of different papers on the use of BEM for UNDEX cavities reveals that most researchers have approached the problem in a similar manner. Where not directly referenced, [Blake 1997a] and particularly [Best, 1993] provide good discussion of the issues involved. There are several steps that many of the reviewed papers mention that are described in the following sections.

4.2.1 Discretization and Boundary Integral Representation

The domain is taken to be the liquid only. Assuming incompressible, irrotational and invisicid flow allows the transformation of the governing equations into a boundary integral formulation. These assumptions relax the physical problem from solving the Navier-Stokes equations throughout a volume to solving the Laplace equation over the volume boundaries.

In order to solve the Laplace equation over the surface of the object, potential flow is used. Potential flow involves introducing a scalar field (the velocity potential, hereafter referred to as simply potential), the gradient of which is the fluid velocity at any point in the domain. This potential field is discretized through a superposition solution, where a collection of functions (singularities) that each satisfy the Laplace equation are distributed over the surface of the object in such a manner as to enforce the fluid boundary conditions. The sum of these singularities also satisfies the Laplace equation, and computational effort is directed at finding the strength of each singularity so boundary conditions are met where required.

The actual discretization of the boundary is similar to finite element techniques and is usually performed by specifying the nodal values of potential or normal derivative of potential, with interpolating elements to specify how the nodal values combine at points on the boundaries that

are not at the nodes. All boundaries of the fluid are discreteized; any air-water surfaces as well all rigid surfaces. In two dimensions, cubic splines seem to be the most common element type, while in 3D, triangles are used. Some papers refer to linear triangles [Chahine 1998], while others refer to higher order elements [Blake 1997a]. Most papers make reference to quadratic or cubic elements, however 3DynaFS (a commercial BEM code from DynaFlow) makes use of linear elements [Chahine].

The solution is subject to free surface and rigid (optionally moving) boundary conditions. The zero normal flow boundary condition restricts fluid velocities to have no normal component (fluid cannot flow through solid boundaries) while the free-surface boundary condition causes the boundaries to move with the local fluid velocity. Initial conditions are specified as either the normal derivative of the potential functions for the rigid boundaries, or as the initial potential for the free surfaces. When discretized as described above, a dense set of linear equations is formed, each equation of which solves the unknown quantity (either potential or normal derivative of potential) at a single node. These values permit subsequent calculation of fluid velocities, which are used to advect the free-surfaces in time.

Although the system is dense, direct solvers are rarely used (although their $O(N^3)$ solution time is used as an example here for lack of a representative iterative value). The most commonly used solver seems to the GMRES solver, [Grilli], [Blake 1997a]. The coefficients of the system that is formed is purely geometric and based on the fluid boundaries. Since it is the unsteady evolution of the boundaries that is of primary interest, the matrices must be reformed and solved at every timestep. Consequently there is no advantage to fully inverting the system to find subsequent solutions to different system right-hand-sides. However the solutions themselves are continuous in time, and because of this, the solution from the previous timestep will be a very good starting point to initialize the solver for the current timestep, hopefully allowing an iterative solver to converge quickly.

One issue arises with distributing and also evaluating the singularities on the boundary. The singularities are, as the name implies, singular (either $1/r$ or $1/r^2$) and cannot be integrated analytically directly. This requires either mathematical tricks (such as a transformation to a cylindrical coordinate system) or numerical quadrature to evaluate the surface integrals required to form the linear system [Lin, 2006]. Accurate evaluation of these weakly singular integrals is very important, since they form the diagonals of the linear system and as such heavily influence the systems numerical conditioning and accuracy of the results.

4.2.2 Bubble Representation

The bubble-contents are represented as an isentropic ideal gas. This allows computation of the internal pressure of the bubble based on the ratio of specific heats, the starting pressure and ratio of current volume to starting volume. The expression for pressure is substituted into the Bernoulli equation to obtain an equation for the time derivative of potential at the bubble surface, which serves to link the pressure of the gas in the bubble to the integral equations. This time derivative is integrated in time throughout the simulation to obtain the current potential at the bubble surface for any timestep. The initial conditions are created from a spherical bubble with an initial radius and internal pressure. Full initial conditions require the potential to be specified over the surface of the bubble and any other free-surfaces. None of the reviewed papers describe how this initial potential is chosen. One possibility may be to work from an initial sphere of the same radius as the bare-charge, with an equal potential to that of the other rigid boundaries, creating stagnant conditions. The pressure inside the bubble would be the pressure of the charge following detonation, but prior to any products expansion.

4.2.3 Main Solver Loop

Once the domain is discretized and the initial conditions set, the solver enters the main time loop. This includes several steps which are summarized below, and described in more detail in [Chahine 1998], [Blake 1997a] and [Tong, ND].

1. The free-surface node positions and surface potentials are integrated in time using one of any number of integration schemes (e.g. Euler [Chahine 1998], Runge-Kutta, Adams-Bashforth [Blake 1997a], etc.).

2. The geometric integrals required to form the boundary integral equation are evaluated, the equations assembled, and solved to yield new values for the normal derivative of potential on free-surfaces and potential on rigid surfaces.

3. From the calculated values in step 2, tangential derivatives of potential on free-surfaces are calculated. How this is done varies slightly between the papers, and is discussed later.

4. The normal and tangential derivatives of potential combine to give the gradient of potential on the free-surface points, which are the fluid velocities at those points. The fluid velocities are used to integrate nodal positions on the free-surface and for determining the time derivatives of potential on the free surface.

5. The volume of the bubble is calculated to determine the new internal pressure, this is not mentioned in any of the UNDEX related papers, but one algorithm [Eberly 2003] is discussed later.

6. The bubble internal pressure and free-surface nodal velocities are used in Bernoulli's equation to determine the time derivative of potential on the free-surfaces.

7. With the time derivative of potential and velocities calculated on the free-surface, the solver returns to step 1.

This loop continues either until the simulation completes, or until a jet forms that pierces the bubble. In the event that the jet pierces the bubble, changes must be made to the discretization by either introducing additional surfaces into the discretization or by adding a vortex ring. This is discussed in a subsequent section. Once the discretization is modified, the solver returns to the main loop and continues.

4.3 Inconsistencies in the Literature

Although the general solver structure seems to be the same through all the papers, there are differences in the implementations. Choices such as element order, methods of integration and handling of jetting vary and are discussed in the following sections.

4.3.1 Tangential Derivatives

The evaluation of tangential derivatives is required to complete the calculation of fluid velocities at the free surfaces. These are in turn used to calculate time derivatives of potential and to integrate node positions in time. Since the two dimensional implementations typically use splines to represent the bubble surface, it is straightforward to evaluate tangential derivatives analytically from the splines.

In three-dimensions, evaluation of the tangential derivatives is somewhat more complex. Several of the papers [Best 1993], [Blake 1997a], [Tong] etc. fit multiquadric surfaces to the area immediately surrounding the node at which tangential derivatives were being evaluated. Derivative calculations are then handled analytically on that surface. In a paper for highly non-linear overturning wave simulation [Grilli 2001] used cubic shape functions to allow analytical evaluation of tangential derivatives, but in a novel way that used adjacent element's nodes rather than increase the resolution of each element. This was done to avoid having to increase the number of nodes in the bubble representation (due to the N^3 solution time issue) while still being able to analytically evaluate tangential derivatives at a high order.

Although not mentioned in the reviewed papers, tangential derivatives could also be evaluated directly from the nodal potential values by projecting the nodal coordinates onto a tangent plane and applying the concepts analogous to the discrete differential operators presented in [Meyer].

Another method of handling would be to use cubic elements that enforce C1 continuity but implemented in an analogous fashion to Catmull-Rom splines. These would not introduce new nodes, but would allow analytic calculation of tangential gradients.

4.3.2 Bubble Jetting

One of the key differences between the reviewed papers is the manner in which jetting is handled. When jetting occurs, one side of the bubble comes into contact with the opposite side. Experimentally this results in a torus shaped bubble, and the same trends are seen in the numerical simulations. However, at the instant that the jet contacts the opposite side of the bubble, the topology of the domain changes, and this introduces issues related to the mathematical model used in the simulation and in the discretization of the simulation.

4.3.2.1 Mathematical Issues

The mathematical issue that is created is that the flowfield being represented transforms from one in which there is zero circulation to one in which there is a finite circulation. This occurs because the two contacting surfaces of the bubble have different surface potentials, which causes a potential jump. This potential jump causes a flowfield similar to the streamlines of a dipole singularity. This is consistent with experiment, but is difficult to represent in simulations.

There are two primary ways of handling this in the literature. The first is to introduce a cut-surface [Best 1993], [Blake 1997a] into the discretization across the jet that contains a potential jump. The magnitude of the potential jump is such that it induces the correct circulation in the flow, while keeping the fluid domain simply connected. This cut surface is then advected using the fluid velocity.

The second approach is to insert a vortex ring [Wang 2005] around the jet (within the bubble), which has a proscribed circulation. This has the same effect as the above method. However it introduces the question of what potential to apply at the contact point, which is strictly speaking, double-valued. One option (the presented option) is to simply use the mean value of the two potentials on either side. What the physical implications of this are unclear from the paper.

Both methods of approaching the mathematical issues simplify the problem by assuming that the jet impact occurs at a point, generally the first point of contact. The potential values at this point are used to determine the appropriate jump condition or circulation values for either the cut-surface or the vortex ring. This is a necessary simplification, since in reality the jet may contact

the opposing cavity wall at many points, or over a surface. Either of these scenarios results in a multivalued jump condition/circulation value, which may violate the flow-irrotationality assumption of potential flow or complicate the remeshing step described in the following section.

4.3.2.2 Discretization Issues

Regardless of whether a vortex ring or cut-surface is used, there are issues related to the discretization of the bubble surface when the jet contacts the opposing wall. At this time, the mesh topology changes from spherical to toroidal [Best 1993], and some remeshing must occur in order to accommodate this. In two dimensions, the two nodes involved in the contact can be removed, and the two opposing surfaces connected. Most papers also refer to a smoothing step in the remeshing procedure to remove sharp discontinuities that might introduce numerical problems.

In three dimensions this process becomes significantly more complex. Unlike the axisymmetric case, the general 3D case does not guarantee that the contact point occurs at two nodes. This combined with mesh variation makes the connection process much more complex. None of the papers reviewed described how to accomplish this, although some made vague references to fully automated systems in three dimensions [Hung 2003].

Another discretization related issue is that of mesh stretching. The jet itself is a relatively fine feature which may be under-resolved if the mesh is coarse. As a result, the tip of the jet will have very high curvature, but likely be represented by only one or two elements, with high angles between them. This will pollute calculations of surface integrals and pose two problems, one for the accuracy of any solutions, and another for the stability of the code if the system formed using these inaccurate values has poor numerical properties. Similarly, splash films [Blake 1997a] and other features with high curvatures will have the same problems albeit probably not to the same degree as the jet itself.

Several papers mention adaptively refining axisymmetric versions of the algorithms by subdividing any segment that exceeds a certain length. This length would logically be calculated to take surface curvature into account to maintain accuracy, but no account of that was mentioned in the papers themselves. In three-dimensions, this problem will worsen, since more panels will be required to represent the bubble to a given accuracy. Assuming an N^3 solution time in the number of nodes, it is likely that accuracy requirements will be relaxed in any three-dimensional implementation below the standards for two-dimensional implementations, and consequently problems related to mesh resolution would be worse. [Hung 2003] claims that adaptive remeshing can introduce instabilities and dramatically affect simulation runtime, and instead prefers an Elastic Mesh Technique proposed by Wang. Again, the papers referring to automation of the three-dimensional implementations did not mention any details of how that remeshing was performed.

4.3.2.3 Conjecture on How to Implement 3D Jetting

The following was not mentioned in any of the papers, but present some ideas on how 3D bubble jetting might be implemented.

By assuming that the impact of the jet occurs at a single point on the opposing wall, the closest node on the opposing wall could be found. The one-ring of elements surrounding these nodes would then be removed, leaving two holes of approximately equal vertex counts. The remeshing step would consist of connecting these two rings together, possibly eliminating one or more extra elements should the number of vertices on each ring be unequal. The nodes that are joined would

either have double valued potentials or have their potential replaced by the mean potential, depending on which scheme from the mathematical issues section was chosen. The resulting mesh would then be smoothed near areas of high curvature.

Another alternative would be to create a volumetric representation of the bubble at the time of impact, and retesselate using something similar to the Marching Cubes algorithm. Mesh simplification and shape-based smoothing would then refine the mesh to have high element quality before proceeding with the simulation.

4.4 Issues Unaddressed by the Reviewed Papers

This section lists some of the things that were not mentioned in the papers reviewed that may pose issues with implementing a BEM UNDEX solver.

4.4.1 Specifying Initial Conditions for a Bubble

The calculation of the internal pressure of the bubble is necessary in order to calculate the time derivative of potential on the free-surfaces. However none of the papers mention a way to do this for an arbitrary closed polyhedron. There are a number of methods in computer graphics literature on how to accomplish this, one of which is presented in [Eberly 2003].

4.4.2 Calculation of Pressures at Boundaries

Only [Blake, 1997a] and [Chahine 1998] make any reference to actually calculating fluid pressures. Integrating the conservation of momentum equation yields Bernoulli's equation, from which a liquid pressure can be found. The paper does not go into any great detail regarding where this pressure is valid, it is presumed everywhere in the fluid domain. Furthermore, by neglecting viscosity potential flow results in zero drag for fully immersed shapes. This phenomenon is referred to as D'Alembert's paradox. Consequently the nature of loadings that can be expected is unclear. [Blake 1997a] does show experimental comparisons, but none appear to be direct pressure trace comparisons.

4.4.3 Incorporation of Cavitation

None of the reviewed papers made any reference to incorporating fluid cavitation into the BEM model. Whether this is a separate area of research, trade secrets, or simply not done is unclear. However cavitation plays a very important role in the overall response of structures to underwater explosions, and its omission would almost certainly compromise results, particularly in the nearfield where structural motion would have the effect of cutting off the incident pressure wave, dramatically reducing the impulsive loads seen by the structure.

One possibility would be to introduce a scattered wave type boundary condition at the wetted surface of the target that essentially acted as a layer between the BEM boundary condition and the finite element load. If the calculated pressure dropped below the vapor pressure, this boundary condition would cut off at the vapor pressure. Rigid boundary conditions in the BEM (prescribed normal derivative of potential) could be reformulated easily to include local structural motion from the finite element code. More sophisticated methods might include a DAA boundary rather than a simple velocity-based scattered wave boundary.

It should be noted that the more sophisticated acoustic element type cavitation modeling (e.g. CFA for the USA code) would be difficult at best to incorporate into a BEM simulation due to the

thickness required for the acoustic layer particularly if jetting and very near field effects were desired.

4.5 Conclusions

Boundary element methods are quite capable of simulating underwater explosion cavities to a reasonable degree of accuracy in many situations. Axisymmetric implementations that take a bubble from initial conditions through to jetting are relatively common, and use one of two approaches for handling the mathematical and discretization challenges that occur. The first approach is to introduce a cut across the jet with a potential jump that causes circulation, and the second is to introduce a vortex ring that accomplishes the same thing. Both approaches require the bubble boundary to be retesselated and smoothed once the jet contacts the opposing side of the bubble. The choice on which approach to use appears to be largely based on who is doing the research, Best and followers advocate the domain cut, while Wang and his followers the vortex ring. Both approaches appear to produce comparable results, and have the same issues for implementation in 3D, although the vortex ring approach may simplify matters somewhat by not advecting an additional surface requiring refinement as the simulation progresses.

By far the most challenging aspect of implementing a jetting 3D UNDEX BEM solver is the retesselation required when the jet contacts the opposing wall. Determining which elements should remain in the mesh, which should be discarded, and how to guarantee element quality are not trivial tasks. Some experimentation may be required to determine an effective scheme.

Other aspects to consider are, the choice of element order, the method of integration (both spatially and temporally) as well as any coupling to an external code and its requirements (e.g. cavitation). Fortunately there is significant variation in the literature regarding these issues, suggesting that a variety of approaches will work well. Similarly, the components of the solver that vary (e.g. choice of element order, integration methods) tend to be very segmented, so different options may be tried without impacting the overall structure of the solver.

5. Summary

The PWA loading analysis option in the Vast-USA interface has been tested using the quarter sphere model. Excellent agreement between the tightly-coupled and loosely-coupled Vast-USA interfaces has been obtained. This has been shown to be the case with no damping and with various forms of damping. Identical results were obtained when using either English or metric units for the model. Although the loading was such that the sphere responds in a linear manner, an analysis was performed using the nonlinear module as well, the latter giving the same results as the linear module. In addition, good agreement was obtained when comparing the Vast-USA analysis with a LS-Dyna-USA analysis of the same sphere. The analysis of the quarter sphere with the diaphragm demonstrated the ability of the tightly-coupled interface to handle cases where there are more structural elements than wetted surface elements.

The DAA1 loading analysis option in the Vast-USA interface has been tested using the quarter cylinder model. Very good agreement between the tightly-coupled and loosely-coupled Vast-USA interfaces has been obtained. Identical results were obtained when using either English or metric units for the model.

The VMA loading analysis option in the Vast-USA interface has been tested using the submerged cylinder model. Reasonably good agreement between the tightly-coupled and loosely-coupled Vast-USA interfaces has been obtained for the case where the model is pinned. The displacement comparison for the unconstrained case was not as good, as there appears to more rigid body drifting in the loosely-coupled results. Perhaps some further study is warranted here. Identical results were obtained when using either English or metric units for the model.

The CPF analyses have demonstrate both the DAA1 and VMA loading analysis options in the Vast-USA interface for a fairly large and complex model. Very good agreement between the tightly-coupled and loosely-coupled Vast-USA interfaces has been obtained. Here the rigid body drifting in the unconstrained model is not as pronounced as in the case of the unconstrained submerged cylinder.

The Suffield circular plate analysis has demonstrated the ability of the Vast-USA interface to accurately predict the structural response of such systems to both shock and bubble induced pressure loading. The results show the importance of including the nonlinear effect, particularly for the bubble pulsating pressure loading. The effect of damping is also evident. The predictions for Shot 1 are closer to experimental results than for Shot 2. Obviously there is a lot more work that could be done here. For example, damping could be modeled more accurately, which would improve the predictions for both shots. Also, it is possible that, in the case of Shot 2, the bubble is too close to the plate for accurate analysis using USA.

The USA interface dialogues for generating the input files for tightly-coupled analyses has proven to be extremely useful in carrying out the various verification and validation analyses described above. As stated, the input files for the USA modules are generated using the keyword format. No effort was made to provide the same capability for the loosely-coupled Vast-USA interface. If use of the latter is to be continued, an attempt should be made to provide a similar automated procedure for it.

The literature review of BEM techniques for UNDEX modeling of bubble dynamics has shown that the extension of the Trident UNDEX software to include such a solver is both doable and

desirable. Since most work to-date has centered on up-to jetting only, it is recommended that the effort concentrate on this aspect of bubble dynamics only. Following this, the much more challenging problem of implementing a jetting UNDEX BEM solver could be tackled.

6. References

Best, J.P., (1993) The formation of toroidal bubbles upon the collapse of transient cavities, Journal of Fluid Mechanics, vol 251, pp. 79-107

Blake, J.R., (1997a) Fluid Dynamics of Underwater Explosions, School of Mathematics and Statistics, University of Birmingham, Research Grant WSFH/U/2060C

Blake, J.R., (1997b) Collapsing cavities, toroidal bubbles and jet impact, Philosophical Transactions of the Royal Society A: Mathematical, Physical and Engineering Sciences, vol 355, Issue 1724, pp. 537-550

Chahine, G.L., (2003) Simulation of surface piercing body coupled response to underwater bubble dynamics using 3DynaFS, a three-dimensional BEM code, Computational Mechanics 32

Chahine, G.L., (2000) Bubble Dynamics Near A Cylindrical Body: 3-D Boundary Element Simulation Of Benchmark Problems, DynaFlow Inc.

Chahine, G.L. (1998) BEM software for free surface flow simulation including fluid-structure interaction effects, International Journal of Computer Applications in Technology, Vol II, Nos 3,4,5

Chahine, G.L., (1997) Numerical Simulation of Cavitation Dynamcs, DynaFlow Inc.

DeRuntz, J.A (1986) Enhanced Analysis Capability in USA-STAGS. Final Report Under Contract N60921-840213, Lockheed Palo Alto Research Laboratory.

Eberly, D., (2003) Polyhedral Mass Properties (Revisited), Geometric Tools, Inc.

Grilli, S. T., (2001) A fully non-linear model for three-dimensional overturning waves over an arbitrary bottom, International Journal for Numerical Methods in Fluids 35

Hung, K.C. (2003) Modeling and Simulation of Explosion Bubble Dynamics and its Effect on Submerged Structure, 74th Shock and Vibration Symposium

Lin, F., (2006) personal communications, Martec Ltd.

Moyer, E.T. Jr., (2003) Another look at UNDEX Bubble Loads, 74th Shock and Vibration Symposium

Meyer, M., (No Date) Discrete Differential-Geometry Operators for Triangulated 2-Manifolds, CalTech

Tong, R. P., (No Date) A boundary Integral Algorithm for Three-Dimensional Bubble Dynamics, School of Mathematics and Statistics, University of Birmingham

Wang, Q.X., (2005) Vortex ring modeling of toroidal bubbles, Journal of Theoretical Computational Fluid Dynamics 00, pp 1-15, published online

Wardlaw, A.W. Jr., (1998) Spherical solutions of an underwater explosion bubble, Shock and Vibration, Vol 5

Zhang, S., (1994) The behavior of a cavitation bubble near a rigid wall, UTAM Symposium on Bubble Dynamics & Interface Phenomena

DOCUMENT CONTROL DATA

(Security classification of title, body of abstract and indexing annotation must be entered when the overall document is classified)

1. ORIGINATOR (the name and address of the organization preparing the document. Organizations for whom the document was prepared, e.g. Centre sponsoring a contractor's report, or tasking agency, are entered in section 8.)

Martec Limited, Suite 400, 1888 Brunswick St., Halifax, NS, B3J 3J8

2. SECURITY CLASSIFICATION (overall security classification of the document including special warning terms if applicable).

UNCLASSIFIED

3. TITLE (the complete document title as indicated on the title page. Its classification should be indicated by the appropriate abbreviation (S,C,R or U) in parentheses after the title).

Improvement and Validation of the Trident UNDEX Interface

4. AUTHORS (Last name, first name, middle initial. If military, show rank, e.g. Doe, Maj. John E.)

Norwood, Merv and Gregson, James

5. DATE OF PUBLICATION (month and year of publication of document)

August 2006

6a. NO. OF PAGES (total containing information Include Annexes, Appendices, etc).

61

6b. NO. OF REFS (total cited in document)

18

7. DESCRIPTIVE NOTES (the category of the document, e.g. technical report, technical note or memorandum. If appropriate, enter the type of report, e.g. interim, progress, summary, annual or final. Give the inclusive dates when a specific reporting period is covered).

CONTRACT REPORT

8. SPONSORING ACTIVITY (the name of the department project office or laboratory sponsoring the research and development. Include address).

Defence R&D Canada – Atlantic
PO Box 1012
Dartmouth, NS, Canada B2Y 3Z7

9a. PROJECT OR GRANT NO. (if appropriate, the applicable research and development project or grant number under which the document was written. Please specify whether project or grant).

Project 11gk16

9b. CONTRACT NO. (if appropriate, the applicable number under which the document was written).

W7707-05-3133

10a ORIGINATOR'S DOCUMENT NUMBER (the official document number by which the document is identified by the originating activity. This number must be unique to this document.)

TN-06-10

10b OTHER DOCUMENT NOs. (Any other numbers which may be assigned this document either by the originator or by the sponsor.)

DRDC Atlantic CR 2006-155

11. DOCUMENT AVAILABILITY (any limitations on further dissemination of the document, other than those imposed by security classification)

(X) Unlimited distribution
( ) Defence departments and defence contractors; further distribution only as approved
( ) Defence departments and Canadian defence contractors; further distribution only as approved
( ) Government departments and agencies; further distribution only as approved
( ) Defence departments; further distribution only as approved
( ) Other (please specify):

12. DOCUMENT ANNOUNCEMENT (any limitation to the bibliographic announcement of this document. This will normally correspond to the Document Availability (11). However, where further distribution (beyond the audience specified in (11) is possible, a wider announcement audience may be selected).

13. ABSTRACT (a brief and factual summary of the document. It may also appear elsewhere in the body of the document itself. It is highly desirable that the abstract of classified documents be unclassified. Each paragraph of the abstract shall begin with an indication of the security classification of the information in the paragraph (unless the document itself is unclassified) represented as (S), (C), (R), or (U). It is not necessary to include here abstracts in both official languages unless the text is bilingual).

This technical note provides a summary of work carried out to improve, verify and validate the Trident UNDEX Interface computer code for DRDC. The improvements included the incorporation of a capability to automatically generate, with minimum input from the user, input files for Vast-USA, and a state-of-the-art survey of potential flow methods for calculating the dynamics of near-field UNDEX gas bubbles. The verification and validation focused on the recently developed tightly coupled Vast-USA interface. In total six different problems were investigated for: (1) comparison with the loosely coupled Vast-USA Interface; (2) comparison with LS-DYNA; (3) comparison with experiment; and (4) consistency with units. Recommendations are made for: (1) further improvements to the Trident UNDEX Interface, including the incorporation of a boundary element technique for modeling near-field UNDEX bubble dynamics; and (2) further verification and validation studies.

14. KEYWORDS, DESCRIPTORS or IDENTIFIERS (technically meaningful terms or short phrases that characterize a document and could be helpful in cataloguing the document. They should be selected so that no security classification is required. Identifiers, such as equipment model designation, trade name, military project code name, geographic location may also be included. If possible keywords should be selected from a published thesaurus. e.g. Thesaurus of Engineering and Scientific Terms (TEST) and that thesaurus-identified. If it not possible to select indexing terms which are Unclassified, the classification of each should be indicated as with the title).

Underwater explosion
Ship structure
Finite element method
Boundary element method
Underwater Shock Analysis
Trident
Warship survivability
Gas bubble
Potential flow
Bubble collapse

This page intentionally left blank.

Defence R&D Canada

Canada's leader in defence
and National Security
Science and Technology

R & D pour la défense Canada

Chef de file au Canada en matière
de science et de technologie pour
la défense et la sécurité nationale

www.drdc-rddc.gc.ca